


PSFC/JA-00-21

Stimulated Radiation from Spatiotemporally Gyrating Relativistic Electron Beams

View metadata, citation and similar papers at core.ac.uk

brought to you by  C
provided by DSpace

J. A. Davies and C. Chen

July, 2000

Plasma Science and Fusion Center
Massachusetts Institute of Technology
Cambridge, MA 02139, USA

This work was supported by the Air Force Office of Scientific Research, Grant No. F49620-97-1-0325 and Grant No. F49620-00-1-0007. Reproduction, translation, publication, use and disposal, in whole or part, by or for the United States government is permitted.

Submitted for publication in *Physics of Plasmas*.

Stimulated Radiation from Spatiotemporally Gyrating Relativistic Electron Beams

J. A. Davies^{a)} and C. Chen
Plasma Science and Fusion Center
Massachusetts Institute of Technology
Cambridge, Massachusetts 02139

ABSTRACT

A stability analysis is made of an electron beam, propagating along and gyrating about a uniform magnetic field, for the case of a spatiotemporal equilibrium distribution in the phase angle of the transverse electron momentum component. The axial momentum component and the magnitude of the transverse momentum component are assumed to have definite values in the equilibrium distribution. The analysis is carried out by applying Lorentz transformations to previous results for nongyrotropic equilibrium distributions. The dispersion matrix, its eigenmodes (which relate field amplitudes), and the dispersion relation are obtained. Numerical results show that varying the spatiotemporal properties of a nongyrotropic equilibrium distribution has only a small effect on maximum growth rates of radiation, but has a strong effect on the frequencies and wave numbers at which instability occurs. A novel mechanism is found by which electrons emit stimulated radiation at frequencies that, in principle, can be greater than the usual Doppler-shifted electron cyclotron frequency by orders of magnitude.

PACS numbers: 42.52.+x, 52.35.Hr, 41.60-m

^{a)} Permanent Address: Department of Physics, Clark University, Worcester, Massachusetts 01610

I. Introduction

Stimulated emission of radiation by electrons gyrating in magnetic fields has been an important subject of theoretical, computational, and experimental investigations in plasma physics, astrophysics, and vacuum electronics for several decades.^{1–6} It is well known that the frequencies of such stimulated radiation correspond to the Doppler-shifted electron cyclotron frequency and its harmonics. For moderately and highly relativistic electrons, the fundamental frequency is approximately $2\gamma_z^2\omega_c$, where γ_z is the relativistic mass factor associated with the axial motion of the electrons and ω_c is the relativistic cyclotron frequency.

A number of papers have dealt with stability properties of a relativistic electron beam in the presence of a uniform magnetic field $\mathbf{B}_0 = B_0\mathbf{e}_z$ for the case of a nonisotropic equilibrium distribution in the phase angle ϕ of the momentum component \mathbf{p}_\perp perpendicular to the field.^{7–14} In particular, it has been suggested that such distributions may be employed to enhance the growth rates of desired radiation modes in devices employing the cyclotron resonance maser instability. More recently, there has been some interest in harmonic conversion processes in spatiotemporal equilibrium distributions in ϕ .^{15–17}

In order to gain a greater understanding of systems with spatiotemporal distributions in ϕ , we analyze the stability properties of such systems in this paper. Preliminary results are given in an earlier report.¹⁸ The analysis is limited to equilibrium distributions in which the axial momentum component p_z and the magnitude of the transverse momentum component \mathbf{p}_\perp have the definite values p_{z0} and $p_{\perp 0}$, respectively. Moreover, the systems are constrained to vary spatially only in the direction of the applied magnetic field (z -direction).

In Ref. 7, we analyzed the stability properties of such electron beam systems for two types of nonisotropic equilibrium distributions in the phase ϕ . These were the time-dependent distribution, which is a function of the equilibrium constant of the motion $\phi - \omega_c t$, and the axial-dependent distribution, which is a function of the equilibrium constant of the motion $\phi - \omega_c z/v_{z0}$.

It is shown in this paper that all relevant spatiotemporal distributions are obtained

from the above distributions by Lorentz transformations. By making use of a Lorentz transformation of the results obtained in Ref. 7, we derive the amplitude equations and dispersion relations for small-amplitude wave perturbations on spatiotemporally gyrating relativistic electron beams. A detailed analysis is made of stability properties of such electron beams.

In the present stability analysis, we find a novel mechanism by which electrons emit stimulated radiation at frequencies that are greater than the usual Doppler-shifted electron cyclotron frequency by orders of magnitude. Two key requirements for this mechanism to occur are that the gyrophases of the electrons in the magnetic field have spatiotemporal correlations, and that the electrons have an inverted population in the transverse momentum space. In contrast to most previous studies of the stimulated radiation by gyrating electrons with a random or spatial-dependent gyrophase distribution and inverted population in the transverse momentum space, the present analysis assumes the gyrophase distribution to form a wave pattern in the direction of the magnetic field. When the phase velocity of the wave pattern is close to the average axial velocity of the electrons, the electrons emit right-hand, circularly polarized stimulated radiation at the relatively high frequency $\omega = 2|\beta_p - \beta_{z0}|^{-1}\omega_c$, where $\beta_p c$ and $\beta_{z0} c$ are the phase and electron axial velocities, respectively, and c is the speed of light in vacuum.

It should be pointed out that the wave pattern in a spatiotemporally gyrating relativistic electron beam depends on how the beam is formed. One of the schemes to form a spatiotemporally gyrating electron beam is through the cyclotron laser (microwave) acceleration.^{19–21} In this case, the phase velocity of the wave pattern in the beam is given by $\beta_p c = \omega_0(\omega_0 - \omega_c)^{-1}\beta_{z0} c$, where ω_0 is the laser (microwave) frequency. In the limit $\omega_0 \gg \omega_c$ and $\beta_{z0} \rightarrow 1$, the stimulated radiation occurs at $\omega \simeq 2\omega_0$.

The organization of this paper is as follows. In Sec. II, the spatiotemporal distribution is described, and the equilibrium distribution is defined in (4). The phase velocity β_p of a surface of constant distribution in phase is defined and evaluated in (9). The primary result of this paper is the dispersion relation for spatiotemporal equilibria with definite values of p_z and p_\perp . This result is stated in (13) of Sec. III. The derivation of our results from the results of Ref. 7 is given in the Appendix. Moreover, equations (A19)-(A21) of

the Appendix give the dispersion matrix for the electron beam systems considered in this paper. Another important result is the expression for the eigenmodes of the amplitude equation given in (19) of Sec. III. This result gives the wave numbers and frequencies of coupled right-hand circularly polarized radiative waves, left-hand circularly polarized radiative waves, and longitudinal electrostatic waves. Numerical examples are presented in Sec. IV. In these examples, the choice of spatiotemporal distribution [namely, the choice of the phase velocity (β_p) of the phase pattern in the equilibrium distribution] is seen to have little effect on maximum growth rates of electromagnetic waves, but to have a strong effect on the range of unstable frequencies and wave numbers and upon the wave numbers and frequencies of coupled waves. These maximum growth rates of electromagnetic waves in the spatiotemporally gyrating relativistic electron beams are greater than those in the corresponding gyrotropic relativistic electron beams. We discuss and summarize our results in Sec. V.

II. Spatiotemporally Gyrating Equilibrium

We consider a beam consisting of electrons moving along and gyrating about a uniform magnetic field $\mathbf{B}_0 = B_0 \hat{\mathbf{e}}_z$. Properties of the system are assumed to vary in the z -direction only. All electrons in the equilibrium beam are assumed to have the same axial momentum ($p_z = p_{z0}$) and the same magnitude of transverse momentum ($p_\perp = p_{\perp 0}$). As shown in Fig. 1, the phase angle of \mathbf{p}_\perp is $\phi = \tan^{-1}(p_y/p_x)$, whereas $\alpha_0 = \tan^{-1}(p_\perp/p_z)$ is the pitch angle. The equilibrium distribution in phase is spatiotemporal; that is, at some $z = z_0$, we impose the condition

$$\phi(z_0, t) = \omega_0 t + \phi_0, \quad (1)$$

where ω_0 and ϕ_0 are constants and t is the time. This geometry is shown in Fig. 2(a). The value of ω_0 depends on how the electron beam is formed. For example, $\omega_0 = 0$ if the electron beam is formed by passing through a tapered static wiggler magnetic field. If the electron beam is generated in a cyclotron resonance accelerator, then ω_0 corresponds to the rf frequency of the accelerator which is a shifted cyclotron frequency. The phase of an unperturbed electron at (z, t) is

$$\phi(z, t) = \omega_0 \left(t - \frac{z - z_0}{v_{z0}} \right) + \phi_0 + \omega_c \frac{z - z_0}{v_{z0}}. \quad (2)$$

In the above equation, the relativistic cyclotron frequency is denoted by $\omega_c = \Omega_c/\gamma_0$, where $\Omega_c = eB_0/mc$ is the nonrelativistic cyclotron frequency, $-e$ and m are respectively the electronic charge and mass, c is the speed of light, $\gamma_0 mc^2$ is the unperturbed relativistic electron energy, and $v_{z0} = p_{z0}/\gamma_0 m$. A spatiotemporally gyrating beam equilibrium is shown schematically in Fig. 2(b). In an experiment, z_0 would correspond to the point where the electron enters the region of interaction with \mathbf{B}_0 . However, boundary conditions are not dealt with in this paper, and the system is considered to extend over the full range (*i.e.*, $-\infty < z < \infty$) of z .

A distribution of values of ϕ at each (z, t) will result if distributions of values of ϕ_0 and/or z_0 exist. From (2), such distributions will produce a distribution in the values of the equilibrium constant of the motion χ defined by

$$\chi = \phi(z, t) - \omega_0 t + (\omega_0 - \omega_c) \frac{z}{v_{z0}}. \quad (3)$$

Consequently, a suitable equilibrium distribution for the system is

$$f_0(p_\perp, p_z, \chi) = n_0 \frac{\delta(p_\perp - p_{\perp 0})}{p_\perp} \delta(p_z - p_{z0}) \Phi(\chi), \quad (4)$$

where $\Phi(\chi)$ is a periodic function of period 2π and n_0 is a constant particle density. We normalize the integral of $f_0(p_\perp, p_z, \chi)$ over momentum space to n_0 . Consequently,

$$\int_0^{2\pi} \Phi(\chi) d\phi = \int_0^{2\pi} \Phi(\chi) d\chi = 1. \quad (5)$$

Two additional constants of the unperturbed motion are

$$\xi = \phi - \omega_c t = \phi - \frac{\Omega_c}{\gamma_0} t, \quad (6)$$

and

$$\zeta = \phi - \omega_c \frac{z}{v_{z0}} = \phi - \frac{m\Omega_c}{p_{z0}} z. \quad (7)$$

Using (3), we express χ as the following linear combination of ξ and ζ :

$$\chi = \frac{\omega_0}{\omega_c} \xi + \left(1 - \frac{\omega_0}{\omega_c}\right) \zeta. \quad (8)$$

If $\omega_0 = \omega_c$ in (8), then $\chi = \xi = \phi - \omega_c t$. In this case, the equilibrium distribution [$f_0(p_\perp, p_z, \chi) = f_0(p_\perp, p_z, \xi)$] in (4) does not depend on z , and we refer to it as the time-dependent equilibrium distribution. If $\omega_0 = 0$ in (8), then $\chi = \zeta = \phi - \omega_c z/v_{z0}$. In this case, the equilibrium distribution [$f_0(p_\perp, p_z, \chi) = f_0(p_\perp, p_z, \zeta)$] in (4) does not depend on t , and we refer to it as the axial-dependent equilibrium distribution.

At each instant of time, there is a z -dependent distribution of phase angles given by (3) and (4). Each point on a surface of constant z will contain the same distribution of values of ϕ . As time progresses, a surface with a given distribution will move with a normalized phase velocity $\beta_p = dz/cdt$ obtained by differentiating (3) with respect to t at constant ϕ . This phase velocity is

$$\beta_p = \frac{\omega_0 \beta_{z0}}{\omega_0 - \omega_c}, \quad (9)$$

where $\beta_{z0} = v_{z0}/c$. Making use of (9), we can also express χ as $\chi = \phi - \omega_c (\beta_{z0} - \beta_p)^{-1} (z/c - \beta_p t)$, which is a single-particle constant of motion. We see that β_p is infinite for the time-dependent equilibrium distribution ($\omega_0 = \omega_c$), and that $\beta_p = 0$ for the axial-dependent equilibrium distribution ($\omega_0 = 0$).

III. Dispersion Relation

A stability analysis of systems with the time-dependent and axial-dependent equilibrium distribution functions has been carried out in Ref. 7. In that analysis, Fourier transforms are taken of the Vlasov and Maxwell's equations in order to derive relations obeyed by the Fourier transforms of the perturbed electric field components. For the case of definite values of $p_z = p_{z0}$ and $p_\perp = p_{\perp 0}$, these are algebraic equations of the form

$$\mathbf{D}(ck, \omega) \mathbf{E}(ck, \omega) = 0, \quad (10)$$

where \mathbf{D} is a three-by-three dispersion matrix and \mathbf{E} is a three-component vector. The components of \mathbf{E} are the Fourier transforms of the perturbed electric field components $E_{1-} = E_{1x} - iE_{1y}$, $E_{1+} = E_{1x} + iE_{1y}$, and E_{1z} . Respectively, these represent the right-hand circularly polarized (RHP) radiative field, the left-hand circular polarized (LHP) radiative field and the longitudinal electric field. The dispersion relation for the system perturbations is given by

$$\det \mathbf{D}(ck, \omega) = 0. \quad (11)$$

It is shown in Appendix A that any spatiotemporal equilibrium distribution with $|\beta_p| < 1$ can be obtained from a Lorentz transformation of the axial-dependent equilibrium distribution, and that any spatiotemporal equilibrium distribution with $|\beta_p| > 1$ can be obtained from a Lorentz transformation of the time-dependent equilibrium distribution. Consequently, a stability analysis of systems with spatiotemporal equilibrium distributions is obtained from Lorentz transformations of (10) and (11). Results for $|\beta_p| < 1$ and $|\beta_p| > 1$ have the same analytic form and are assumed to extend to the case of $|\beta_p| = 1$.

The primary result of this paper (derived in Appendix B) is the dispersion relation for systems having definite values of $p_\perp = p_{\perp 0}$ and $p_z = p_{z0}$. In terms of the dimensionless wavenumber \hat{k} and the dimensionless frequency $\hat{\omega}$ defined by

$$\begin{aligned} \hat{k} &= \frac{ck}{\omega_c}, \\ \hat{\omega} &= \frac{\omega}{\omega_c}, \end{aligned} \quad (12)$$

the dispersion relation can be expressed as

$$\begin{aligned}
M_{--}(\hat{k}, \hat{\omega}) M_{++}(\hat{k}, \hat{\omega}) M_{zz}(\hat{k}, \hat{\omega}) = & \\
\frac{1}{2} \left(\frac{\omega_p^2}{\omega_c^2} \right)^2 \beta_{\perp 0}^2 |s_1|^2 \left\{ (\beta_{z0} \hat{\omega} - \hat{k})^2 M_{++}(\hat{k}, \hat{\omega}) + [\beta_{z0} (\hat{\omega} - 2\beta_p \hat{k}_0) - (\hat{k} - 2\hat{k}_0)]^2 M_{--}(\hat{k}, \hat{\omega}) \right\} & \\
+ \frac{1}{4} \left(\frac{\omega_p^2}{\omega_c^2} \right)^2 \beta_{\perp 0}^4 |s_2|^2 \left[\hat{\omega} (\hat{\omega} - 2\beta_p \hat{k}_0) - \hat{k} (\hat{k} - 2\hat{k}_0) \right]^2 M_{zz}(\hat{k}, \hat{\omega}) & \\
- \frac{1}{4} \left(\frac{\omega_p^2}{\omega_c^2} \right)^3 \beta_{\perp 0}^4 (s_2 s_{-1}^2 + s_{-2} s_1^2) \left[\hat{\omega} (\hat{\omega} - 2\beta_p \hat{k}_0) - \hat{k} (\hat{k} - 2\hat{k}_0) \right] & \\
\times [\beta_{z0} (\hat{\omega} - 2\beta_p \hat{k}_0) - (\hat{k} - 2\hat{k}_0)] (\beta_{z0} \hat{\omega} - \hat{k}), & \quad (13)
\end{aligned}$$

which is a tenth-degree polynomial equation in either \hat{k} or $\hat{\omega}$. In equation (13),

$$\begin{aligned}
M_{--}(\hat{k}, \hat{\omega}) &= (\hat{\omega}^2 - \hat{k}^2) (\hat{\omega} - \hat{k} \beta_{z0} - 1)^2 - \frac{\omega_p^2}{\omega_c^2} (\hat{\omega} - \hat{k} \beta_{z0}) (\hat{\omega} - \hat{k} \beta_{z0} - 1) \\
&+ \frac{1}{2} \frac{\omega_p^2}{\omega_c^2} \beta_{\perp 0}^2 (\hat{\omega}^2 - \hat{k}^2), \\
M_{++}(\hat{k}, \hat{\omega}) &= \left[(\hat{\omega} - 2\beta_p \hat{k}_0)^2 - (\hat{k} - 2\hat{k}_0)^2 \right] (\hat{\omega} - \hat{k} \beta_{z0} - 1)^2 \\
&- \frac{\omega_p^2}{\omega_c^2} (\hat{\omega} - \hat{k} \beta_{z0} - 2) (\hat{\omega} - \hat{k} \beta_{z0} - 1) \\
&+ \frac{1}{2} \frac{\omega_p^2}{\omega_c^2} \beta_{\perp 0}^2 \left[(\hat{\omega} - 2\beta_p \hat{k}_0)^2 - (\hat{k} - 2\hat{k}_0)^2 \right], \\
M_{zz}(\hat{k}, \hat{\omega}) &= (\hat{\omega} - \hat{k} \beta_{z0} - 1)^2 - \frac{\omega_p^2}{\omega_c^2} (1 - \beta_{z0}^2). \quad (14)
\end{aligned}$$

Moreover, $\omega_p^2 = 4\pi n_0 e^2 / \gamma_0 m$, $\beta_{\perp 0} = p_{\perp 0} / \gamma_0 m c$,

$$\hat{k}_0 = c k_0 / \omega_c = (\beta_p - \beta_{z0})^{-1}, \quad (15)$$

and

$$s_n = \int_0^{2\pi} d\chi \Phi(\chi) \exp(-in\chi). \quad (16)$$

Notice that $\beta_p \hat{k}_0 = \omega_0 / \omega_c - 1$, where ω_0 is defined in (1).

The dispersion relation in (13) is invariant under the transformation

$$\begin{aligned}
\hat{k} &\longrightarrow -\hat{k}^* + 2\hat{k}_0, \\
\hat{\omega} &\longrightarrow -\hat{\omega}^* + 2\beta_p \hat{k}_0. \quad (17)
\end{aligned}$$

Under the transformation in (17), the $\Re(\hat{k})$ -, $\Re(\hat{\omega})$ -plane is inverted through the point $(\hat{k}_0, \beta_p \hat{k}_0)$, and $\Im(\hat{k})$ and $\Im(\hat{\omega})$ are unchanged. Consequently, a plot of $\Im(\hat{\omega})$ as a function of real \hat{k} is unchanged by reflection through the vertical line $\hat{k} = \hat{k}_0$.

It follows from (A15) of Appendix B that the eigenmodes of the dispersion matrix for the case of a spatiotemporal equilibrium distribution are given in terms of the electric field by

$$\begin{aligned} \mathbf{E}(z, t) = e^{i(kz - \omega t)} [2^{-1/2} E_{1-}(k, \omega) \hat{\mathbf{e}}_+ + 2^{-1/2} E_{1+}(k - 2k_0, \omega - 2\omega_0) \hat{\mathbf{e}}_- e^{-2i(k_0 z - \omega_0 t)} \\ + E_{1z}(k - k_0, \omega - \omega_0) \hat{\mathbf{e}}_z e^{-i(k_0 z - \omega_0 t)}], \end{aligned} \quad (18)$$

where

$$\mathbf{E}(\hat{k}, \hat{\omega}) = \begin{pmatrix} E_{1-}(\hat{k}, \hat{\omega}) \\ E_{1+}(\hat{k} - 2\hat{k}_0, \hat{\omega} - 2\beta_p \hat{k}_0) \\ E_{1z}(\hat{k} - \hat{k}_0, \hat{\omega} - \beta_p \hat{k}_0) \end{pmatrix}. \quad (19)$$

For positive $\Re(\hat{k})$, $E_{1-}(\hat{k}, \hat{\omega})$ and $E_{1+}(\hat{k}, \hat{\omega})$ are Fourier transforms of the right hand circularly polarized (RHP) and the left hand circularly polarized (LHP) radiation fields, respectively. [These polarization assignments are reversed for negative $\Re(\hat{k})$.] The transform $E_{1z}(\hat{k}, \hat{\omega})$ is that of the longitudinal electric field.

IV. Numerical Examples

In all of the following numerical examples, the value chosen for $\Phi(\chi)$ in (4) is

$$\Phi(\chi) = \lim_{\epsilon \rightarrow 0} \delta(\chi - \epsilon), \quad 0 \leq \chi \leq 2\pi. \quad (20)$$

Consequently, all equilibrium electrons with the same z and t have the same phase ϕ . For these distributions, a system is stable for sufficiently large magnitudes of real \hat{k} . The corresponding Fourier components in (16) are $s_1 = s_2 = 1$. In all examples, $\omega_p^2/\omega_c^2 = 0.05$ and $\alpha_0 = 0.4$, where $\alpha_0 = \tan^{-1}(p_{\perp 0}/p_{z0})$ is the equilibrium pitch angle.

Figure 3 shows growth-rate curves [$\Im(\hat{\omega}) = \Im(\omega)/\omega_c$ vs. $\hat{k} = ck/\omega_c$ with k real] for a system with $\gamma_0 = 2.0$ (and the corresponding normalized axial velocity $\beta_{z0} = 0.7977$). The resonance condition for the cyclotron maser instability is satisfied at $\hat{k} = (1 - \beta_{z0})^{-1} = 4.94$. Plots are shown for several values of the normalized phase velocity β_p . Figures 3(a) and 3(d) refer respectively to the axial-dependent ($\beta_p = 0$, or $\omega_0 = 0$) and time-dependent ($\beta_p = \infty$, or $\omega_0 = \omega_c$) distributions. The corresponding values of $\hat{k}_0 = (\beta_p - \beta_{z0})^{-1}$ in (15) are -1.254 and zero, respectively. Figure 3(c) pertains to $\beta_p = 2.0$ (or $\omega_0 = 1.663\omega_c$) with $\hat{k}_0 = 0.8317$, whereas Fig. 3(b) pertains to $\beta_p = 0.85$ (or $\omega_0 = 16.24\omega_c$) with $\hat{k}_0 = 19.11$.

It is interesting to point out that the maximum growth rate for each of the nonisotropic phase distributions in Figs. 3(a)-3(d) is greater than the maximum growth rate for the corresponding gyrotropic relativistic electron beam, which is $\Im(\hat{\omega}) \simeq 0.054$. (See Fig. 4 of Ref. 7.)

Reference to Fig. 3 shows that maximum growth rates and growth rates at the resonance value $\hat{k} = 4.94$ are not very sensitive to the value of the phase velocity β_p . On the other hand, the range of values of \hat{k} for which instability exists may be very sensitive to values of β_p . (A corresponding sensitivity of the range of unstable frequencies is present because, for unstable modes, $\Re(\hat{\omega}) \simeq \beta_{z0}\hat{k}$ when $\hat{k} \gg 1$.) In particular, instability of an RHP radiative component will occur at large values of \hat{k} [and of $\Re(\hat{\omega})$] if $\hat{k}_0 = (\beta_p - \beta_{z0})^{-1}$ is large in magnitude. This effect is illustrated in Fig. 3(b) where $\hat{k}_0 = 19.11$. The effect is explained by first noting that instability is expected for values of \hat{k} near the resonance \hat{k} and second recalling (from the discussion at the end of Sec. III) that plots of $\Im(\omega)$ vs. real

\hat{k} are symmetric under reflection through \hat{k}_0 . It is also a consequence of the fact [evident from (19)] that frequencies and wavenumbers of coupled waves in an eigenmode become greatly divergent for large \hat{k}_0 .

In Fig. 3 and in the following Figs. 4-9, both wide and narrow solid curves are employed. Detailed numerical calculations of roots of the dispersion relation in (13) show that the wide curves refer to modes whose instability, in the low wavenumber region ($\hat{k} < \hat{k}_0$), is due to coupling of the cyclotron mode with the electromagnetic modes with $\omega \pm ck = 0$. In the high wavenumber region ($\hat{k} > \hat{k}_0$), the instability is due to coupling of the cyclotron mode with the electromagnetic modes with $\omega - 2\beta_{z0}ck_0 \pm c(k - 2k_0) = 0$. The wide curves are characterized by $\omega - \beta_{z0}ck - \omega_c \simeq 0$ over the entire \hat{k} -interval of instability. The narrow solid curves refer to modes whose instability is due to coupling of the electrostatic modes. They are characterized by $\omega - \beta_{z0}ck - \omega_c + \frac{\omega_p}{\omega_c} (1 - \beta_{z0}^2)^{1/2} \simeq 0$ over intervals of instability with $\hat{k} < \hat{k}_0$ and $\omega - \beta_{z0}ck - \omega_c - \frac{\omega_p}{\omega_c} (1 - \beta_{z0}^2)^{1/2} \simeq 0$ over intervals of instability with $\hat{k} > \hat{k}_0$.

Figures 4(a) and 4(b) are, respectively, plots of $\Re(\hat{\omega})$ vs. \hat{k} and of $\Im(\hat{\omega})$ vs. \hat{k} over the interval of the upper- \hat{k} growth-rate peak in Fig. 3(b). Coupled radiative components of the field amplitude eigenvector in (19) are $E_{1-}(\hat{k}, \hat{\omega})$ and $E_{1+}(\hat{k} - 2\hat{k}_0, \hat{\omega} - 2\beta_p\hat{k}_0) = E_{1+}(\hat{k} - 38.21, \hat{\omega} - 32.48)$. Consequently, $E_{1-}(\hat{k}, \hat{\omega})$ represents high-frequency, forward-traveling, RHP radiation, whereas $E_{1+}(\hat{k} - 38.21, \hat{\omega} - 32.48)$ represents low-frequency radiation in the \hat{k} -interval in Fig. 4. It is evident from Fig. 4(a) that the high-frequency radiation is slow-wave radiation (*i. e.*, its wave phase velocity $c\hat{\omega}/\hat{k}$ is less than the speed of light).

It is of interest to determine the relative contributions of the high- and low- frequency components to the total Poynting flux. As a measure of the relative contribution of the high-frequency component to the total Poynting flux, we employ the Poynting flux ratio $\mathcal{S}_{\mathcal{R}}$ defined by

$$\mathcal{S}_{\mathcal{R}} = \left| \frac{\langle S_{-z}(ck, \omega) \rangle}{\langle S_{-z}(ck, \omega) + S_{+z}(ck - 2ck_0, \omega - 2\beta_pck_0) \rangle} \right|. \quad (21)$$

In the above equation, $\langle S_{-z}(ck, \omega) \rangle$ and $\langle S_{+z}(ck - 2ck_0, \omega - 2\beta_pck_0) \rangle$ are the time-averaged z -components of the Poynting fluxes produced by the high-frequency and low-

frequency electromagnetic components, respectively. [Because the low-frequency flux may be backward traveling for some intervals of \hat{k} , the ratio $\mathcal{S}_{\mathcal{R}}$ may exceed one and will approach infinity when high- and low-frequency fluxes cancel.] An expression for $\mathcal{S}_{\mathcal{R}}$ as a function of \hat{k} and $\hat{\omega}$ is presented in (A31) of Appendix C.

A plot of $\log_{10} \mathcal{S}_{\mathcal{R}}$ vs. \hat{k} for the system of Figs. 3(b) and 4 is presented in Fig. 5. We regard the high-frequency component as dominant if $\mathcal{S}_{\mathcal{R}} > 1/2$ [*i.e.*, if $\log_{10} \mathcal{S}_{\mathcal{R}} > -0.3010$]. Figure 5 shows that this condition is valid over the interval $37 < \hat{k} < 40$, which corresponds to $30\omega_c < \Re(\omega) < 33\omega_c$ in Fig. 4(a). It is to be emphasized that these wavenumbers and frequencies greatly exceed the resonance frequency and wavenumber for the cyclotron maser instability ($\hat{\omega} = \hat{k} = 4.94$). The frequency ω_0 (equal to $16.24\omega_c$ in this example) is exceeded by approximately a factor of two.

The rapid variations in the value of $\mathcal{S}_{\mathcal{R}}$ in the interval $37 < \hat{k} < 40$ are explained as follows. Reference to (A29) shows that $S_{+z}(ck - 2ck_0, \omega - 2\beta_p ck_0)$ vanishes when $ck = 2ck_0$ ($\hat{k} = 38.21$) and when $\Re(\omega) = 2\beta_p ck$ [$\Re(\hat{\omega}) = 32.48$ and $\hat{k} = 39.6$ for the unstable branch associated with the highest maximum of the growth-rate peak in Fig. 4(b)]. At these values of \hat{k} , $\log_{10} \mathcal{S}_{\mathcal{R}} = 0$. For values of \hat{k} between these zeros of the low-frequency flux, $S_{+z}(ck - 2ck_0, \omega - 2\beta_p ck_0)$ becomes negative, allowing $\log_{10} \mathcal{S}_{\mathcal{R}}$ to approach infinity when the high-frequency and low-frequency fluxes cancel.

Next we consider mildly relativistic systems with $\gamma_0 = 1.2$ and the corresponding $\beta_{z0} = 0.50914$. Resonance for the cyclotron maser instability occurs at $\hat{\omega} = \hat{k} = 2.037$. Figures 6(a) and 6(b) show growth-rate [$\Im(\hat{\omega})$ vs. \hat{k}] curves for the cases of $\beta_p = 0$ ($\hat{k}_0 = -1.9644$ and $\omega_0 = 0$) and $\beta_p = 0.67580$ ($\hat{k}_0 = 6$ and $\omega_0/\omega_c = 4.0548$). From (19), coupled radiative modes for the case of $\beta_p = 0$ [Fig. 6(a)] are $E_{1-}(\hat{k}, \hat{\omega})$ and $E_{1+}(\hat{k} + 3.9288, \hat{\omega})$. Figure 7 is a plot of $\Re(\omega)$ vs. \hat{k} for unstable modes in this case. It is evident from this plot that the highest frequency of unstable modes is approximately $2.1\omega_c$.

In Figs. 8(a) and 8(b), we present, respectively, plots of $\Re(\omega)$ vs. \hat{k} and $\Im(\omega)$ vs. \hat{k} of unstable modes when $\beta_p = 0.67580$ for the \hat{k} interval of the large- \hat{k} growth peak in Fig. 6(b). Coupled radiative components, obtained from (19), in this case are $E_{1-}(\hat{k}, \hat{\omega})$ and $E_{1+}(\hat{k} - 12, \hat{\omega} - 8.1096)$. From Fig. 8(a), it is evident that growing electromagnetic waves with frequencies of approximately $7\omega_c$ are present in this system.

Figure 9 is a plot of the logarithm of the Poynting ratio in (21) as a function of \hat{k} over the interval of \hat{k} in Fig. 8. It is evident that the high-frequency RHP flux dominates the low frequency flux (*i.e.* $\log_{10} \mathcal{S}_{\mathcal{R}} > -0.3010$) over a very narrow interval in this case. Numerical results show this interval to be $11.987 \leq \hat{k} \leq 12.036$ with $7.079 \leq \Re(\hat{\omega}) \leq 7.103$. These values are much greater than the resonance values of $\hat{\omega} = \hat{k} = 2.037$ given above for the cyclotron resonance maser instability. Moreover, the values $7.079 \leq \Re(\hat{\omega}) \leq 7.103$ are slightly less than twice the value $\omega_0/\omega_c = 4.0548$.

The above and other numerical examples indicate that the width of the interval of relatively large high-frequency flux decreases with increasing frequency (increasing \hat{k}_0) and with decreasing γ_0 .

V. Conclusions

In Ref. 7, stability properties of an electron beam, propagating in a uniform magnetic field $\mathbf{B}_0 = B_0 \hat{\mathbf{e}}_z$, were analyzed under the constraint that all quantities depend spatially only on z . The equilibrium distribution in the phase angle ϕ of \mathbf{p}_\perp was assumed to be nonrandom, and two distributions were considered. These were the time-dependent distribution in which the distribution depends on ϕ through the constant of the unperturbed motion $\xi = \phi - \omega_c t$ and the axial-dependent distribution in which the distribution depends on ϕ through the constant of the unperturbed motion $\zeta = \phi - \omega_c z/v_{z0}$. In this paper the analysis has been extended to spatiotemporal distributions, which depend on the constant of the unperturbed motion $\chi = \phi - \omega_0 t + (\omega_0 - \omega_c)z/v_{z0}$, defined in (3). This analysis is limited to equilibrium distributions [equation (4)] for which p_z and p_\perp have definite values.

By carrying out Lorentz transformations of the results of Ref. 7, we have obtained the dispersion relation in (13) for the spatiotemporal equilibrium distribution. The dispersion matrix is given in (A19)-(A21), and its eigenmodes (which describe the coupling of the RHP radiative, LHP radiative, and electrostatic waves) are given in (19). The parameters which define this spatiotemporal system are p_{z0} , $p_{\perp 0}$, ω_p^2/ω_c^2 , β_p , s_1 , and s_2 . The parameter β_p is the phase velocity of surfaces (normal to the z -axis) upon which the equilibrium distribution in ϕ has a fixed form. The Fourier components s_1 and s_2 are given by (16). Once $\Phi(\chi)$ (and consequently s_1 and s_2) are fixed, the spatiotemporal distribution can still be changed by varying β_p , where $0 \leq |\beta_p| \leq \infty$.

Numerical computations indicate that the above variation in β_p has little effect on maximum growth rates or on the growth rate at the resonance frequency for the cyclotron-resonance maser instability. However, it has a strong effect on the range of real ω and real k of RHP radiation over which the system is unstable, and has a strong effect on the relative wave numbers and frequencies of coupled RHP radiative, LHP radiative, and electrostatic waves. In particular, the distribution in (20) has been shown to result in unstable modes in which the RHP radiative component dominates over a relatively narrow frequency range at much higher frequencies than the resonance frequency for the cyclotron-maser instability. These high frequencies occur when the phase velocity β_p is close to the beam velocity β_{z0} .

In such cases, these frequencies exceed ω_0 by approximately a factor of two.

It is well known that the cyclotron maser instability in a gyrotropic beam is very sensitive to axial velocity spread if the instability occurs at a highly Doppler upshifted cyclotron frequency.²³ The parameter regime of interest here is $\beta_p \simeq \beta_{z0} < 1$. In this case, the dispersion relations for the system are a set of coupled integral equations if there is an axial momentum spread. (The integral equations are obtained by applying the Lorentz transformation to the integral equations in Eqs. (41)-(43) of Ref. 7.) We have begun an analysis of the properties of these integral equations in order to determine the degree to which thermal spread affects the instability reported in this paper.

Acknowledgment

This work was supported in part by the Air Force Office of Scientific Research, Grant Nos. F49620-97-0325 and F49620-00-1-0007.

Appendix: Derivation of Dispersion Relations and the Poynting Flux Ratio

A. Lorentz Transformations of Spatiotemporal Equilibrium Distributions

Consider a Lorentz transformation from an initial frame of reference S to a frame S' which moves with the normalized velocity β_u in the positive z -direction relative to S . Under this transformation,

$$\begin{aligned} z' &= \gamma_u (z - \beta_u ct), & p'_{z0} &= \gamma_u (p_{z0} - \beta_u \gamma_0 mc), & ck' &= \gamma_u (ck - \beta_u \omega), \\ ct' &= \gamma_u (ct - \beta_u z), & \gamma'_0 mc &= \gamma_u (\gamma_0 mc - \beta_u p_{z0}), & \omega' &= \gamma_u (\omega - \beta_u ck), \end{aligned} \quad (A1)$$

where $\gamma_u = (1 - \beta_u^2)^{-1/2}$. The quantities $\phi' = \phi$ and $p'_{\perp 0} = p_{\perp 0}$ are invariant under this transformation. The distribution function in (4) is also invariant.²² Expressed in terms of primed quantities, it is

$$\begin{aligned} f'_0(p'_\perp, p'_z, \chi) &= f_0(p_\perp, p_z(p'_\perp, p'_z), \chi) = \\ &= n'_0 \frac{\delta(p'_\perp - p'_{\perp 0})}{p'_\perp} \delta(p'_z - p'_{z0}) \Phi(\chi), \end{aligned} \quad (A2)$$

where $n'_0 = n_0 \gamma'_0 / \gamma_0$.

Using (3) and the Lorentz transformations in (A1), we obtain the following expression for χ in terms of primed quantities:

$$\begin{aligned} \chi &= \frac{1}{\beta'_{z0} + \beta_u} \left(\frac{\omega'_0}{\omega'_c} \beta'_{z0} + \beta_u \right) \xi' + \frac{\beta'_{z0}}{\beta'_{z0} + \beta_u} \left(1 - \frac{\omega'_0}{\omega'_c} \right) \zeta', \\ \xi' &= \phi - \omega'_c t', \\ \zeta' &= \phi - \omega'_c \frac{z'}{v'_{z0}}. \end{aligned} \quad (A3)$$

Quantities appearing in (A3) are $\omega'_c = eB_0 / \gamma'_0 mc$ and $\omega'_0 = \omega_0 / \gamma_u$. The phase velocity β'_p of surfaces of constant ϕ (or constant distribution in ϕ) relative to the reference frame S' is determined by differentiating (A3) with respect to t' at constant ϕ . The result, written in terms of both primed and unprimed quantities is

$$\beta'_p = \frac{\omega'_0 \beta'_{z0} + \omega'_c \beta_u}{\omega'_0 - \omega'_c} = \frac{\omega_0 (\beta_{z0} - \beta_u) + \omega_c \beta_u}{\omega_0 (1 - \beta_u \beta_{z0}) - \omega_c}. \quad (A4)$$

The transformation velocity β_u from a general reference frame S to a frame S' relative to which the distribution is time-dependent is obtained by setting the coefficient of ζ' in

(A3) equal to zero and solving for β_u . Expressing the result in terms of unprimed quantities and employing (9), we obtain

$$\beta_u = \frac{1}{\beta_p}. \quad (A5)$$

Consequently, the transformation is possible if (relative to S) $|\beta_p| > 1$. Conversely, if a distribution is time-dependent relative to S' , then $|\beta_p| > 1$ relative to any other reference frame S .

Similarly, the transformation velocity β_u from a general reference frame S to a frame S' relative to which the distribution is axial-dependent is obtained by setting the coefficient of ξ' in (A3) equal to zero and solving for β_u . The result is

$$\beta_u = \beta_p. \quad (A6)$$

Consequently, the transformation is possible if (relative to S) $|\beta_p| < 1$. Conversely, if a distribution is axial-dependent relative to S' , then $|\beta_p| < 1$ relative to any other reference frame S .

B. Derivation of the Dispersion Matrix and Eigenmodes

In the stability analysis of Ref. 7 for the time-dependent and axial-dependent equilibrium distributions, the Fourier transforms of the field components $\mathbf{E}'(ck', \omega')$ were found to be related by matrix equations of the form

$$\mathbf{D}'(ck', \omega') \mathbf{E}'(ck', \omega') = 0, \quad (A7)$$

where \mathbf{D}' is a three by three dispersion matrix and \mathbf{E}' is a three-component column matrix whose components are Fourier transforms of $E'_{1-} = E'_{1x} - iE'_{1y}$, $E'_{1+} = E'_{1x} + iE'_{1y}$, and $E_1 z'$. The primes appear in these equations because the frame of reference in which the distribution is either time-dependent or axial-dependent is defined as the primed frame (S') in this treatment.

i. Derivation for the case of $|\beta_p| > 1$

The time-dependent equilibrium distribution function is given by (A2) with $\chi = \xi'$. From the discussion in Sec. A of this appendix, it is clear that properties of a system

with a spatiotemporal equilibrium distribution and $|\beta_p| > 1$ can be derived from Lorentz transformations of a system with a time-dependent equilibrium distribution. It is shown in Ref. 7 that for the time-dependent equilibrium distribution the eigenmode $\mathbf{E}'(k', \omega')$ is of the form

$$\mathbf{E}'(ck', \omega') = \begin{pmatrix} E_{1-}(ck', \omega') \\ E_{1+}(ck', \omega' - 2\omega'_c) \\ E_{1z}(ck', \omega' - \omega'_c) \end{pmatrix}, \quad (\text{A8})$$

where $\omega'_c = eB_0/\gamma'_0 mc$. The dispersion matrix for the time-dependent case is readily derived from (59) of Ref. 7. In order to determine stability properties of systems with spatiotemporal equilibrium distributions with phase velocities $|\beta_p| > 1$, it is necessary to apply the Lorentz transformation to the quantities appearing in (A7). Under the Lorentz transformation from S' to S (which travels with velocity $-\beta_u$ relative to S'), the electromagnetic fields (and their Fourier transforms) transform as

$$\begin{aligned} E_{1z} &= E'_{1z} & B_{1z} &= B'_{1z} \\ E_{1x} &= \gamma_u (E'_{1x} + \beta_u B'_{1y}) & B_{1x} &= \gamma_u (B'_{1x} - \beta_u E'_{1y}) \\ E_{1y} &= \gamma_u (E'_{1y} - \beta_u B'_{1x}) & B_{1y} &= \gamma_u (B'_{1y} + \beta_u E'_{1x}) \end{aligned} \quad (\text{A9})$$

From (19) and the Maxwell equation

$$\frac{\partial}{\partial z'} E'_{1\pm}(z', t') = \pm \frac{\partial}{\partial t'} B'_{1\pm}(z', t'), \quad (\text{A10})$$

where $B'_{1\pm}(z', t') = B'_{1x}(z', t') \pm iB'_{1y}(z', t')$, we find that under the Lorentz transformation,

$$E_{1\pm}(ck, \omega) = \gamma_u \left(1 + \frac{\beta_u ck'}{\omega'} \right) E'_{1\pm}(ck', \omega'). \quad (\text{A11})$$

It follows from (A9) and (A11) that the transformation rule for the eigenvector $\mathbf{E}(ck', \omega')$ in (A7) and (A8) is

$$\mathbf{E}(ck, \omega) = \mathbf{L}(ck', \omega') \mathbf{E}'(ck', \omega'), \quad (\text{A12})$$

where

$$\mathbf{L}(ck', \omega') = \begin{pmatrix} \gamma_u \left(1 + \frac{\beta_u ck'}{\omega'} \right) & 0 & 0 \\ 0 & \gamma_u \left(1 + \frac{\beta_u ck'}{\omega' - 2\omega'_c} \right) & 0 \\ 0 & 0 & 1 \end{pmatrix}, \quad (\text{A13})$$

and

$$\mathbf{E}(ck, \omega) = \begin{pmatrix} E_{1-}(ck, \omega) \\ E_{1+}(ck - 2\beta_u \gamma_u \omega'_c, \omega - 2\gamma_u \omega'_c) \\ E_{1z}(ck - \beta_u \gamma_u \omega'_c, \omega - \gamma_u \omega'_c) \end{pmatrix}. \quad (\text{A14})$$

Using (A5) and the Lorentz transformations in (A1), we can rewrite the arguments in the above expression entirely in terms of quantities pertaining to S to obtain

$$\mathbf{E}(ck, \omega) = \begin{pmatrix} E_{1-}(ck, \omega) \\ E_{1+}(ck - 2ck_0, \omega - 2\beta_p ck_0) \\ E_{1z}(ck - ck_0, \omega - \beta_p ck_0) \end{pmatrix}, \quad (\text{A15})$$

where

$$ck_0 = \frac{\omega_c}{\beta_p - \beta_{z0}}. \quad (\text{A16})$$

By comparing (A7) and (A12), it is seen that the dispersion matrix in the unprimed (spatiotemporal) system is given by

$$\mathbf{D}(ck, \omega) = \mathbf{L}(ck', \omega') \mathbf{D}'(ck', \omega') \mathbf{L}^{-1}(ck', \omega'). \quad (\text{A17})$$

An expression, obtained from (A1) and (A13), that is useful in the evaluation of (A17) is

$$\mathbf{L}^{-1}(ck', \omega') = \begin{pmatrix} \gamma_u \left(1 - \frac{\beta_u ck}{\omega}\right) & 0 & 0 \\ 0 & \gamma_u \left[1 - \beta_u \frac{ck - 2\beta_u \gamma_u \omega'_c}{\omega - 2\gamma_u \omega'_c}\right] & 0 \\ 0 & 0 & 1 \end{pmatrix}. \quad (\text{A18})$$

The dispersion matrix for spatiotemporal equilibrium distributions is determined using (59) from Ref. 7, (A13), (A17), and (A18). When β_u is eliminated from the result by using (A5), we obtain

$$\mathbf{D}(ck, \omega) = \begin{pmatrix} D_{--}(ck, \omega) & -\eta_{-+} & -\eta_{-z} \\ -\eta_{+-} & D_{++}(ck - 2ck_0, \omega - 2\beta_p ck_0) & -\eta_{+z} \\ -\eta_{z-} & -\eta_{z+} & D_{zz}(ck - ck_0, \omega - \beta_p ck_0) \end{pmatrix}. \quad (\text{A19})$$

The diagonal terms in the above equation are:

$$D_{--}(ck, \omega) = \omega^2 - c^2 k^2 - \frac{\omega_p^2}{2} \left[2 \left(\omega - \frac{kp_{z0}}{\gamma_0 m} \right) \left(\omega - \frac{kp_{z0}}{\gamma_0 m} - \omega_c \right)^{-1} - \frac{p_{\perp 0}^2}{\gamma_0^2 m^2 c^2} (\omega^2 - c^2 k^2) \left(\omega - \frac{kp_{z0}}{\gamma_0 m} - \omega_c \right)^{-2} \right],$$

$$\begin{aligned}
D_{++}(ck - 2ck_0, \omega - 2\beta_p ck_0) &= (\omega - 2\beta_p ck_0)^2 - (ck - 2ck_0)^2 \\
&\quad - \frac{\omega_p^2}{2} \left[2 \left(\omega - \frac{kp_{z0}}{\gamma_0 m} - 2\omega_c \right) \left(\omega - \frac{kp_{z0}}{\gamma_0 m} - \omega_c \right)^{-1} \right. \\
&\quad \left. - \frac{p_{\perp 0}^2}{\gamma_0^2 m^2 c^2} [(\omega - 2\beta_p ck_0)^2 - (ck - 2ck_0)^2] \left(\omega - \frac{kp_{z0}}{\gamma_0 m} - \omega_c \right)^{-2} \right], \\
D_{zz}(ck - ck_0, \omega - \beta_p ck_0) &= 1 - \omega_p^2 \left(1 - \frac{p_{z0}^2}{\gamma_0^2 m^2 c^2} \right) \left(\omega - \frac{kp_{z0}}{\gamma_0 m} - \omega_c \right)^{-2}. \quad (A20)
\end{aligned}$$

The terms $D_{--}(ck, \omega)$, $D_{++}(ck, \omega)$, and $D_{zz}(ck, \omega)$ are respectively the dispersion functions for the RHP radiative field, the LHP radiative field, and the longitudinal electric field.

The off-diagonal elements of the dispersion matrix in (A19) are

$$\begin{aligned}
\eta_{-+} &= -\frac{\omega_p^2}{2} s_2 \frac{p_{\perp 0}^2}{\gamma_0^2 m^2 c^2} \frac{\omega}{\omega - 2\beta_p ck_0} \\
&\quad \times [\omega(\omega - 2\beta_p ck_0) - ck(ck - 2ck_0)] \left(\omega - \frac{kp_{z0}}{\gamma_0 m} - \omega_c \right)^{-2}, \\
\eta_{-z} &= -\omega_p^2 \omega s_1 \frac{p_{\perp 0}}{\gamma_0 mc} \left(\frac{p_{z0}}{\gamma_0 mc} \omega - ck \right) \left(\omega - \frac{kp_{z0}}{\gamma_0 m} - \omega_c \right)^{-2}, \\
\eta_{+-} &= -\frac{\omega_p^2}{2} s_{-2} \frac{p_{\perp 0}^2}{\gamma_0^2 m^2 c^2} \frac{\omega - 2\beta_p ck_0}{\omega} \\
&\quad \times [\omega(\omega - 2\beta_p ck_0) - ck(ck - 2ck_0)] \left(\omega - \frac{kp_{z0}}{\gamma_0 m} - \omega_c \right)^{-2}, \\
\eta_{+z} &= -\omega_p^2 (\omega - 2\beta_p ck_0) s_{-1} \frac{p_{\perp 0}}{\gamma_0 mc} \\
&\quad \times \left[\frac{p_{z0}}{\gamma_0 mc} (\omega - 2\beta_p ck_0) - (ck - 2ck_0) \right] \left(\omega - \frac{kp_{z0}}{\gamma_0 m} - \omega_c \right)^{-2}, \\
\eta_{z-} &= -\frac{\omega_p^2}{2} \omega^{-1} s_{-1} \frac{p_{\perp 0}}{\gamma_0 mc} \left(\frac{p_{z0}}{\gamma_0 mc} \omega - ck \right) \left(\omega - \frac{kp_{z0}}{\gamma_0 m} - \omega_c \right)^{-2}, \\
\eta_{z+} &= -\frac{\omega_p^2}{2} (\omega - 2\beta_p ck_0)^{-1} s_1 \frac{p_{\perp 0}}{\gamma_0 mc} \\
&\quad \times \left[\frac{p_{z0}}{\gamma_0 mc} (\omega - 2\beta_p ck_0) - (ck - 2ck_0) \right] \left(\omega - \frac{kp_{z0}}{\gamma_0 m} - \omega_c \right)^{-2}. \quad (A21)
\end{aligned}$$

In the above equation, $\omega_p^2 = 4\pi n_0 e^2 / \gamma_0 m$ is the relativistic plasma frequency squared. This quantity is invariant under Lorentz transformations. The quantities s_n are the Fourier

series coefficients of $\Phi(\chi)$ defined by

$$s_n = \int_0^{2\pi} d\chi \Phi(\chi) \exp(-in\chi). \quad (\text{A22})$$

ii. Derivation for the Case of $|\beta_p| < 1$

Properties of systems having a spatiotemporal equilibrium distribution with phase velocity $|\beta_p|$ less than one are determined by carrying out Lorentz transformations of results for the axial-dependent equilibrium distribution. The axial-dependent equilibrium distribution (for definite values of $p'_{\perp 0}$ and p'_{z0}) is attained by setting $\chi = \zeta'$ in (A2). In this case, the dispersion matrix \mathbf{D}' in (A7) is readily obtained from (90) of Ref. 7. The eigenmode \mathbf{E}' in (A7), given by (91) of Ref. 7, is

$$\mathbf{E}'(ck', \omega') = \begin{pmatrix} E'_{1-}(ck', \omega') \\ E'_{1+}\left(ck' + 2\frac{\omega'_c}{\beta'_{z0}}, \omega'\right) \\ E'_{1z}\left(ck' + \frac{\omega'_c}{\beta'_{z0}}, \omega'\right) \end{pmatrix}. \quad (\text{A23})$$

Equation (A12) governs the Lorentz transformation of the eigenvector from S' (frame of the axial-dependent equilibrium distribution) to S (the frame of the spatiotemporal equilibrium distribution). From (A1), (A9), and (A11), it is seen that now the transformation matrix \mathbf{L} is given by

$$\mathbf{L}(ck', \omega') = \begin{pmatrix} \gamma_u \left(1 + \frac{\beta_u ck'}{\omega'}\right) & 0 & 0 \\ 0 & \gamma_u \left(1 + \beta_u \frac{ck' + 2\omega'_c/\beta'_{z0}}{\omega'}\right) & 0 \\ 0 & 0 & 1 \end{pmatrix}. \quad (\text{A24})$$

The transformed eigenvector is obtained from (A12). When written in terms of β_u , the expression for this eigenvector differs from that in (A14). However, once (A6) is employed to set $\beta_u = \beta_p$, the expression for $\mathbf{E}(ck, \omega)$ is the same as (A15). Consequently, (A15) gives the eigenmodes $\mathbf{E}(ck, \omega)$ for spatiotemporal equilibrium distributions both for $|\beta_p| > 1$ and for $|\beta_p| < 1$.

Equation (A17) together with (A24) is used to obtain $\mathbf{D}(ck, \omega)$, the dispersion matrix for the case of the spatiotemporal equilibrium distribution with $|\beta_p| < 1$. After (A6) is used to eliminate reference to β_u and unprimed quantities are eliminated, the result is the

same as that given by (A19)-(A21) for the case of $|\beta_p| > 1$. Consequently, (A19)-(A21) gives the dispersion matrix for the spatiotemporal equilibrium distribution for both the cases of $|\beta_p| > 1$ and of $|\beta_p| < 1$.

iii. The case of $\beta_p = 1$

Equations (A15) for the eigenmodes and (A19)-(A21) are well behaved in the limit of $|\beta_p| = 1$. Consequently, we consider them to be valid when $|\beta_p| = 1$. The fact that $|\beta_p| = 1$ corresponds to $|\beta_u| = 1$ causes no difficulty, because such quantities as γ_0 , $p_{\perp 0}$, and p_{z0} are held fixed while the limit is taken.

To summarize, for all $-\infty < \beta_p < \infty$, the dispersion matrix for the case of spatiotemporal equilibrium distributions is given by (A19)-(A21) and the eigenmodes are of the form given by (A15). The dispersion relation in (13) is obtained by setting the determinant of the matrix in (A19) equal to zero. [It can also be obtained by substituting Lorentz transformed quantities into the dispersion relations in (69) and (100) of Ref. 7 and replacing the transformation velocity with the appropriate function of β_p .]

C. Derivation of the Poynting Flux Ratio

In the analysis of the numerical results in Sec. IV, we employed the Poynting flux ratio $\mathcal{S}_{\mathcal{R}}$ in (21), which is the magnitude of the ratio of the z -component of the average Poynting flux of the RHP radiation field to the z -component of the average total Poynting flux. For a single eigenmode (A15) of the dispersion matrix in (A19), the Poynting flux vector is

$$\mathbf{S} = \frac{c}{4\pi} \Re(\mathbf{E}) \times \Re(\mathbf{B}), \quad (\text{A25})$$

where

$$\begin{aligned} \mathbf{E}(z, t) = & \\ & \hat{\mathbf{e}}_+ 2^{-1/2} E_{1-}(ck, \omega) \exp(ikz - i\omega t) + \\ & \hat{\mathbf{e}}_- 2^{-1/2} E_{1+}(ck - 2ck_0, \omega - 2\beta_p ck_0) \exp[i(k - 2k_0)z - i(\omega - 2\beta_p ck_0)t] + \\ & \hat{\mathbf{e}}_z E_{1z}(ck - ck_0, \omega - \beta_p ck_0) \exp[i(k - k_0)z - i(\omega - \beta_p ck_0)t], \end{aligned} \quad (\text{A26})$$

with

$$\hat{\mathbf{e}}_{\pm} = 2^{-1/2} (\hat{\mathbf{e}}_{\mathbf{x}} \pm i\hat{\mathbf{e}}_{\mathbf{y}}). \quad (\text{A27})$$

Application of the Maxwell equation in (A10) yields

$$\begin{aligned} \mathbf{B}(\mathbf{x}, t) = & \\ & \hat{\mathbf{e}}_+ 2^{-1/2} B_{1-}(ck, \omega) \exp(ikz - i\omega t) + \\ & \hat{\mathbf{e}}_- 2^{-1/2} B_{1+}(ck - 2ck_0, \omega - 2\beta_p ck_0) \exp[i(k - 2k_0)z - i(\omega - 2\beta_p ck_0)t], \end{aligned}$$

where

$$\begin{aligned} B_{1-}(ck, \omega) &= -i \frac{ck}{\omega} E_{1-}(ck, \omega), \\ B_{1+}(ck - 2ck_0, \omega - 2\beta_p ck_0) &= i \frac{(ck - 2ck_0)}{(\omega - 2\beta_p ck_0)} E_{1+}(ck - 2ck_0, \omega - 2\beta_p ck_0). \end{aligned} \quad (\text{A28})$$

Substituting (A27) and (A28) into the z -component of (A25), averaging the result over the time interval $T = \pi/(\Re(\omega) - \beta_p ck_0)$, and assuming that

$$|2\pi\Im(\omega)| \ll |\Re(\omega) - \beta_p ck_0|, \quad (\text{A29})$$

we obtain the time averaged z -component of the Poynting vector $\langle S_z \rangle$. The result is

$$\begin{aligned} \langle S_z \rangle = & \frac{c}{8\pi} \exp(2\Im(\omega)t) \left[ck \frac{\Re(\omega)}{|\omega|^2} \frac{1}{2} E_{1-}(ck, \omega) E_{1-}^*(ck, \omega) \right. \\ & + (ck - 2ck_0) \frac{(\Re(\omega) - 2\beta_p ck_0)}{|\omega - 2\beta_p ck_0|^2} \\ & \left. \times \frac{1}{2} E_{1+}(ck - 2ck_0, \omega - 2\beta_p ck_0) E_{1+}^*(ck - 2ck_0, \omega - 2\beta_p ck_0) \right]. \end{aligned} \quad (\text{A30})$$

It follows from (A30) that the value of the Poynting flux ratio $\mathcal{S}_{\mathcal{R}}$ in (21) is

$$\begin{aligned} \mathcal{S}_{\mathcal{R}} = & \left| \frac{\langle S_{-z}(ck, \omega) \rangle}{\langle S_{-z}(ck, \omega) + S_{+z}(ck - 2ck_0, \omega - 2\beta_p ck_0) \rangle} \right| = \\ & \left| \frac{ck \Re(\omega) |\omega - 2\beta_p ck_0|^2 \left[|\omega|^2 (ck - 2ck_0) (\Re(\omega) - 2\beta_p ck_0) RR^* + ck \Re(\omega) |\omega - 2\beta_p ck_0|^2 \right]^{-1}}{\hat{k} \Re(\hat{\omega}) |\hat{\omega} - 2\beta_p \hat{k}_0|^2 \left[|\hat{\omega}|^2 (\hat{k} - 2\hat{k}_0) (\Re(\hat{\omega}) - 2\beta_p \hat{k}_0) RR^* + \hat{k} \Re(\hat{\omega}) |\hat{\omega} - 2\beta_p \hat{k}_0|^2 \right]^{-1}} \right|, \end{aligned} \quad (\text{A31})$$

where

$$R = \frac{E_{1+}(ck - 2ck_0, \omega - 2\beta_p ck_0)}{E_{1-}(ck, \omega)}. \quad (A32)$$

The amplitude ratio in (A32) is obtained from the amplitude (eigenvector) equation in (12). The flux ratio in (A31) can exceed one and may approach infinity at particular values of k .

References

1. R. C. Davidson, *Physics of Nonneutral Plasmas* (Addison-Wesley, Reading, Massachusetts, 1990) Ch. 7.
2. R. O. Twiss, *Aust. J. Phys.* **11**, 564 (1958).
3. J. Schneider, *Phys. Rev. Lett.* **2**, 504 (1959).
4. A. V. Gapunov, Addendum, *Izv. VUZ. Radiafiz.* **2**, 837 (1959).
5. J. L. Hirshfield and J. M. Wachtel, *Phys. Rev. Lett.* **2**, 533 (1964).
6. K. E. Kreischer, T. Kimura, B. G. Danly, and R. J. Temkin, *Phys. Plasmas* **4**, 1907 (1997).
7. J. A. Davies and C. Chen, *Phys. Plasmas* **5**, 3416 (1998).
8. A. Fruchtman and L. Friedland, *J. Appl. Phys.* **53**, 4011 (1982).
9. A. Fruchtman and L. Friedland, *IEEE J. Quantum Electron.* **19**, 327 (1983).
10. A. Fruchtman, *Phys. Fluids B* **4**, 4101 (1992).
11. H. P. Freund, J. Q. Dong, C. S. Wu, and L. C. Lee, *Phys. Fluids* **30**, 3106 (1987).
12. T. H. Kho, A. T. Lin, and L. Chen, *Phys. Fluids* **31**, 3120 (1988).
13. C. Chen, J. A. Davies, G. Zhang, and J. Wurtele, *Phys. Rev. Lett.* **69**, 73 (1992).
14. C. Chen, B. G. Danly, G. Shevets, and J. S. Wurtele, *IEEE Trans. Plasma Sci.* **20**, 149 (1992).
15. C. S. Kou, D. B. McDermott, N. C. Luhmann, and K. R. Chu, *IEEE Trans. Plasma Sci.* **18**, 343 (1990).
16. J. L. Hirshfield, *Phys. Rev. A* **44**, 6845 (1991); *Phys. Rev. A* **46**, 1561 (1992).
17. A. K. Ganguly and J. L. Hirshfield, *Phys. Rev. Lett.* **70**, 291 (1993); *Phys. Rev. E* **47**, 4364 (1993).
18. J. A. Davies and C. Chen, *Proc. SPIE, Intense Microwave Pulses V* **3702**, Howard E. Brandt, Ed., 88 (1999).
19. C. Chen, *Phys. Rev. A* **46**, 6654 (1992).
20. M. A. LaPointe, R. B. Yoder, C. Wang, A. K. Ganguly, and J. L. Hirshfield, *Phys. Rev. Lett.* **76**, 2718 (1996).
21. R. Pakter, R. Schneider, and F. B. Rizzato, *Phys. Rev. E.* **49**, 1594 (1994).

22. S. R. de Groot, W. A. van Leeuwen, and Ch. G. van Weert, *Relativistic Kinetic Theory* (North Holland, Amsterdam, New York, Oxford, 1980) 4.
23. R. C. Davidson and P. H. Yoon, Phys. Rev. A **39**, 2534 (1989).

Figure Captions

- Fig. 1. The phase angle ϕ and pitch angle α_0 of a single-particle momentum \mathbf{p} .
- Fig. 2. (a) The generation of a spatiotemporally gyrating relativistic electron beam equilibrium with electrons arriving at $z = z_0$ with a gyrophase of $\phi(z_0, t) = \omega_0 t + \phi_0$. (b) A spatiotemporally gyrating relativistic electron beam equilibrium.
- Fig. 3. Plots of $\Im(\hat{\omega}) = \Im(\omega)/\omega_c$ vs. $\hat{k} = ck/\omega_c$ (real) for equilibrium parameters $\gamma_0 = 2$, $\omega_p^2/\omega_c^2 = 0.05$, $\alpha_0 = 0.4$, and $s_1 = s_2 = 1$. The corresponding value of $\beta_{z0} = 0.79766$. Values of the normalized phase velocity β_p and \hat{k}_0 are: (a) $\beta_p = 0$ ($\omega_0 = 0$) and $\hat{k}_0 = -1.2537$, (b) $\beta_p = 0.85$ ($\omega_0 = 16.24\omega_c$) and $\hat{k}_0 = 19.11$, (c) $\beta_p = 2$ ($\omega_0 = 1.663\omega_c$) and $\hat{k}_0 = 0.8317$, and (d) $\beta_p = \infty$ ($\omega_0 = \omega_c$) and $\hat{k}_0 = 0$. Wide lines indicate that instability is due to coupling of a cyclotron mode. Narrow lines indicate that instability is due to coupling of an electrostatic mode.
- Fig. 4. Dispersion relations in the region of the higher- \hat{k} growth peak for the system of Fig. 3b, with equilibrium parameters $\gamma_0 = 2$, $\omega_p^2/\omega_c^2 = 0.05$, $\alpha_0 = 0.4$, $s_1 = s_2 = 1$, and $\beta_p = 0.85$ ($\omega_0 = 16.24\omega_c$). The corresponding values of β_{z0} and \hat{k}_0 are 0.7977 and 19.11, respectively. Plots are (a) $\Re(\hat{\omega}) = \Re(\omega)/\omega_c$ vs. $\hat{k} = ck/\omega_c$ (real) for unstable modes, and (b) $\Im(\hat{\omega})$ vs. \hat{k} (real). Frequencies and wavenumbers refer to the component $E_-(ck, \omega)$. The second radiative component of the eigenvector is $E_+(ck - 38.21\omega_c, \omega - 32.48\omega_c)$. Wide lines indicate that instability is due to coupling of a cyclotron mode. Narrow lines indicate that instability is due to coupling of an electrostatic mode.
- Fig. 5. Plots of the Poynting ratio $\mathcal{S}_{\mathcal{R}}$ in (A31) vs. $\hat{k} = ck/\omega_c$ for unstable modes in the region of the higher- \hat{k} growth peak for the system of Fig. 3(b), 4(a), and 4(b). Wide lines indicate that instability is due to coupling of a cyclotron mode. Narrow lines indicate that instability is due to coupling of an electrostatic mode.
- Fig. 6. Growth rate curves [$\Im(\hat{\omega}) = \Im(\omega)/\omega_c$ vs. $\hat{k} = ck/\omega_c$ (real)] for the equilibrium parameters $\gamma_0 = 1.2$, $\omega_p^2/\omega_c^2 = 0.05$, $\alpha_0 = 0.4$, $s_1 = s_2 = 1$, and the corresponding value $\beta_{z0} = 0.5091$. In plot (a), $\beta_p = 0$ ($\omega_0 = 0$) and $\hat{k}_0 = -1.964$; whereas in plot (b), $\beta_p = 0.67580$ ($\omega_0 = 4.055\omega_c$) and $\hat{k}_0 = 6$. Frequencies and wavenumbers refer to the

component $E_-(ck, \omega)$. The second radiative component of the eigenvector in (19) is $E_+(ck - \hat{k}_0\omega_c, \omega - \beta_p\hat{k}_0\omega_c)$. Wide lines indicate that instability is due to coupling of a cyclotron mode. Narrow lines indicate that instability is due to coupling of an electrostatic mode.

Fig. 7. Plot of $\Re(\hat{\omega})$ vs. \hat{k} (real) for unstable modes of the system of Fig. 6(a). Frequencies and wavenumbers refer to the component $E_-(ck, \omega)$. The second radiative component of the eigenvector in (19) is $E_+(ck + 3.929\omega_c, \omega)$. Wide lines indicate that instability is due to coupling of a cyclotron mode. Narrow lines indicate that instability is due to coupling of an electrostatic mode.

Fig. 8. Dispersion relations in the region of the higher- \hat{k} growth peak for the system of Fig. 6(b), with equilibrium parameters $\gamma_0 = 1.2$, $\omega_p^2/\omega_c^2 = 0.05$, $\alpha_0 = 0.4$, $s_1 = s_2 = 1$, and $\beta_p = 0.6758$ ($\omega_0 = 4.055\omega_c$). The corresponding values of β_{z0} and \hat{k}_0 are 0.50914 and 6, respectively. Plots are (a) $\Re(\hat{\omega}) = \Re(\omega)/\omega_c$ vs. $\hat{k} = ck/\omega_c$ (real) for unstable modes, and (b) $\Im(\hat{\omega})$ vs. \hat{k} (real). Frequencies and wavenumbers refer to the component $E_-(ck, \omega)$. The second radiative component of the eigenvector in (19) is $E_+(ck - 12\omega_c, \omega - 8.110\omega_c)$. Wide lines indicate that instability is due to coupling of a cyclotron mode. Narrow lines indicate that instability is due to coupling of an electrostatic mode.

Fig. 9. Plots of the Poynting ratio $\mathcal{S}_{\mathcal{R}}$ in (A31) vs. $\hat{k} = ck/\omega_c$ for unstable modes in the region of the higher- \hat{k} growth peak for the system of Fig. 6(b). Wide lines indicate that instability is due to coupling of a cyclotron mode. Narrow lines indicate that instability is due to coupling of an electrostatic mode.

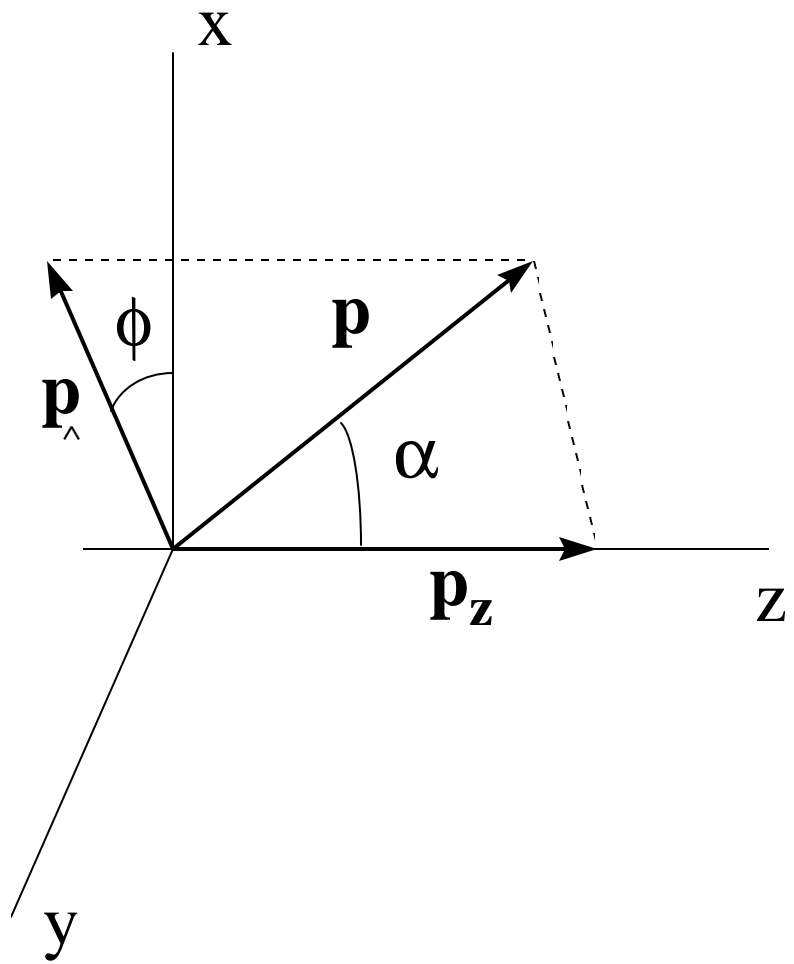


Fig. 1

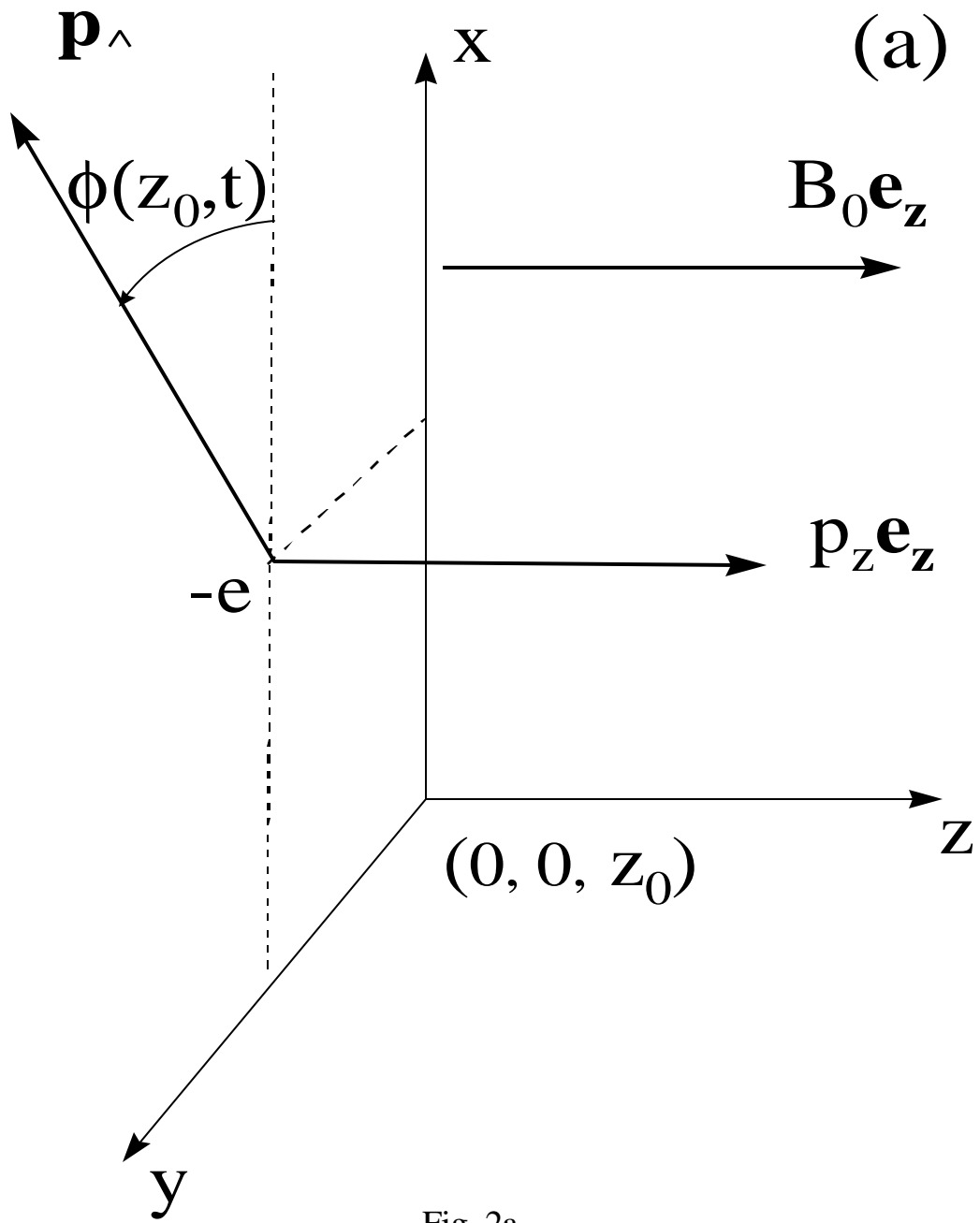


Fig. 2a

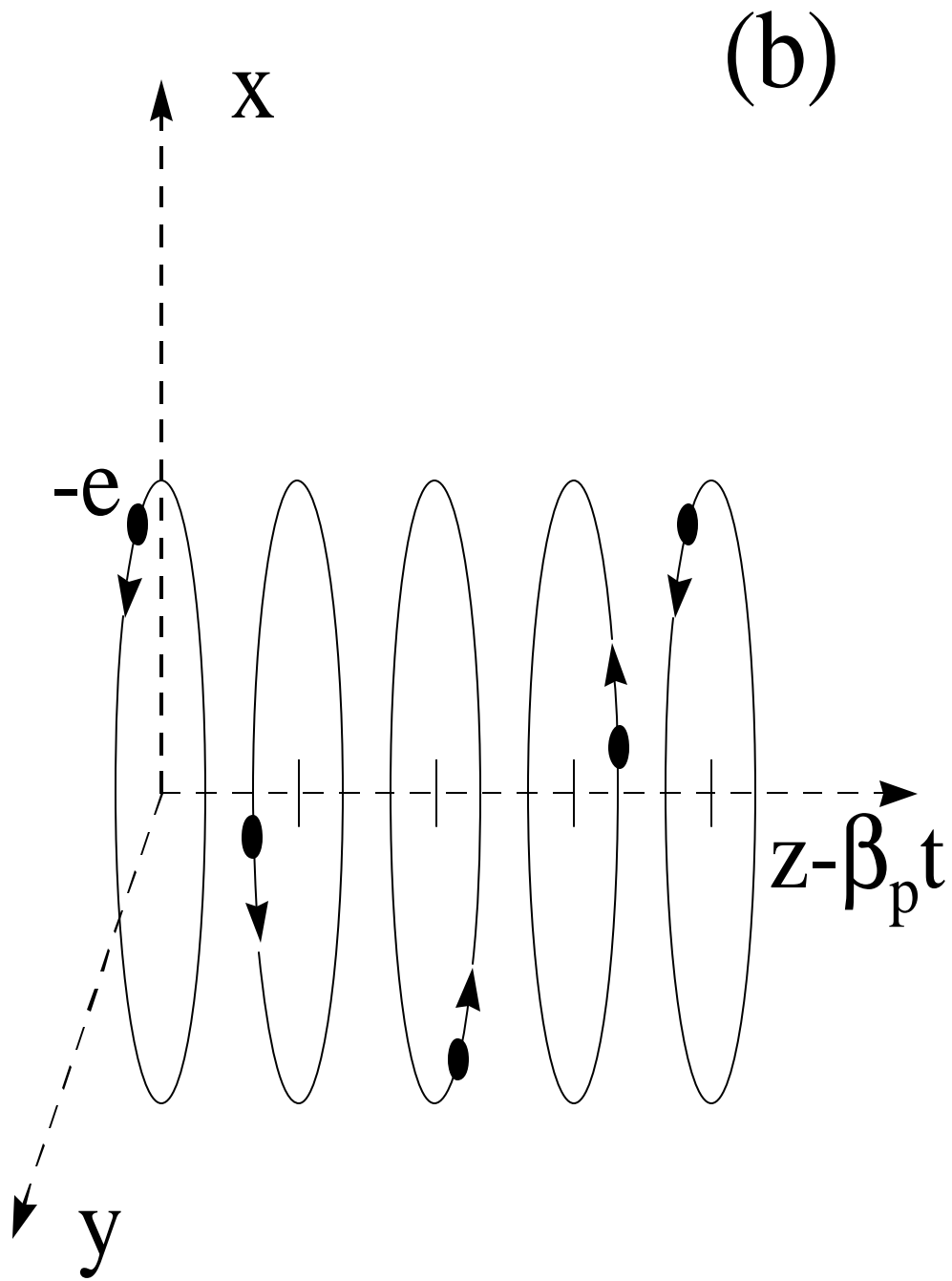


Fig. 2b

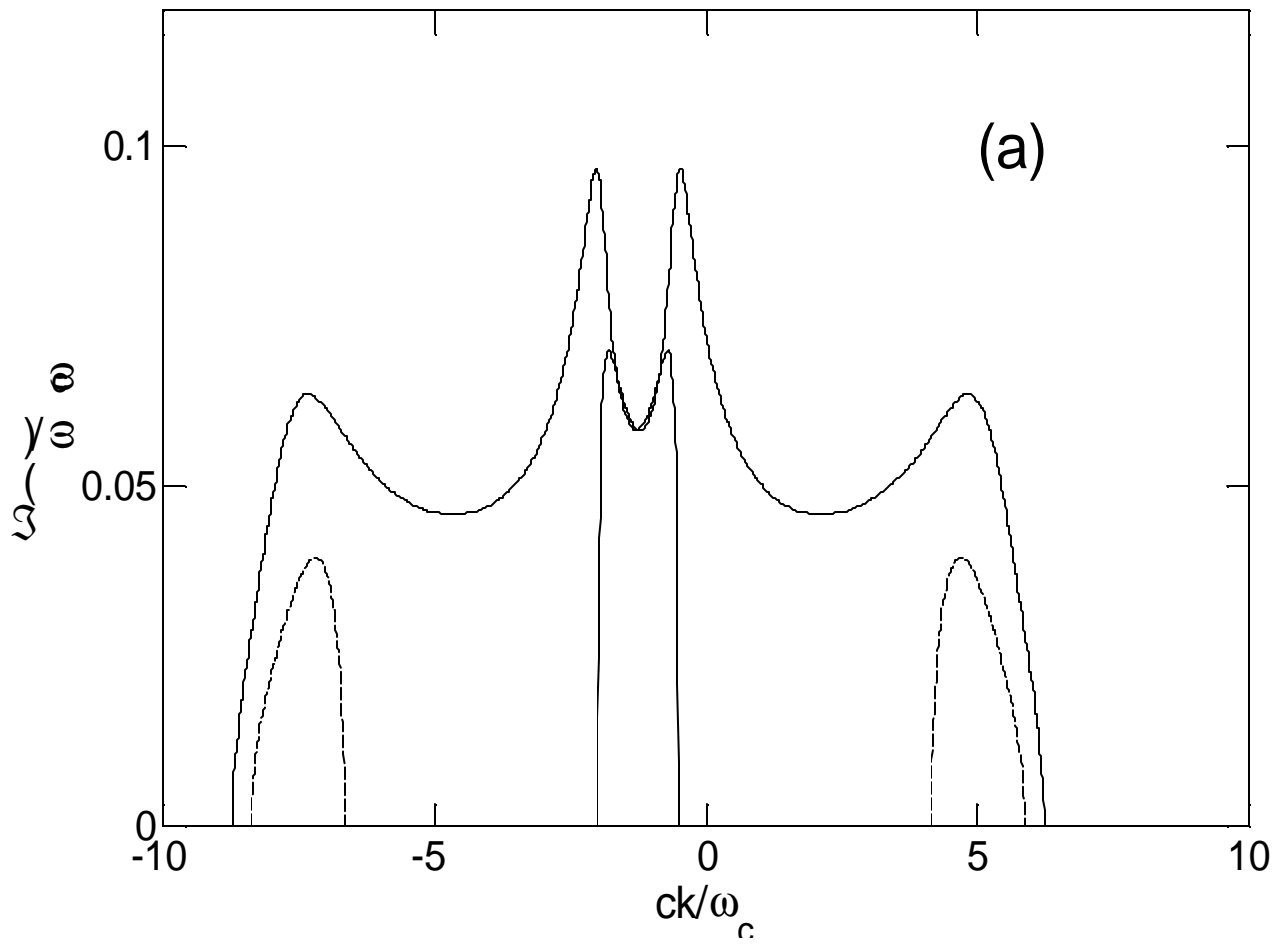


Fig. 3a

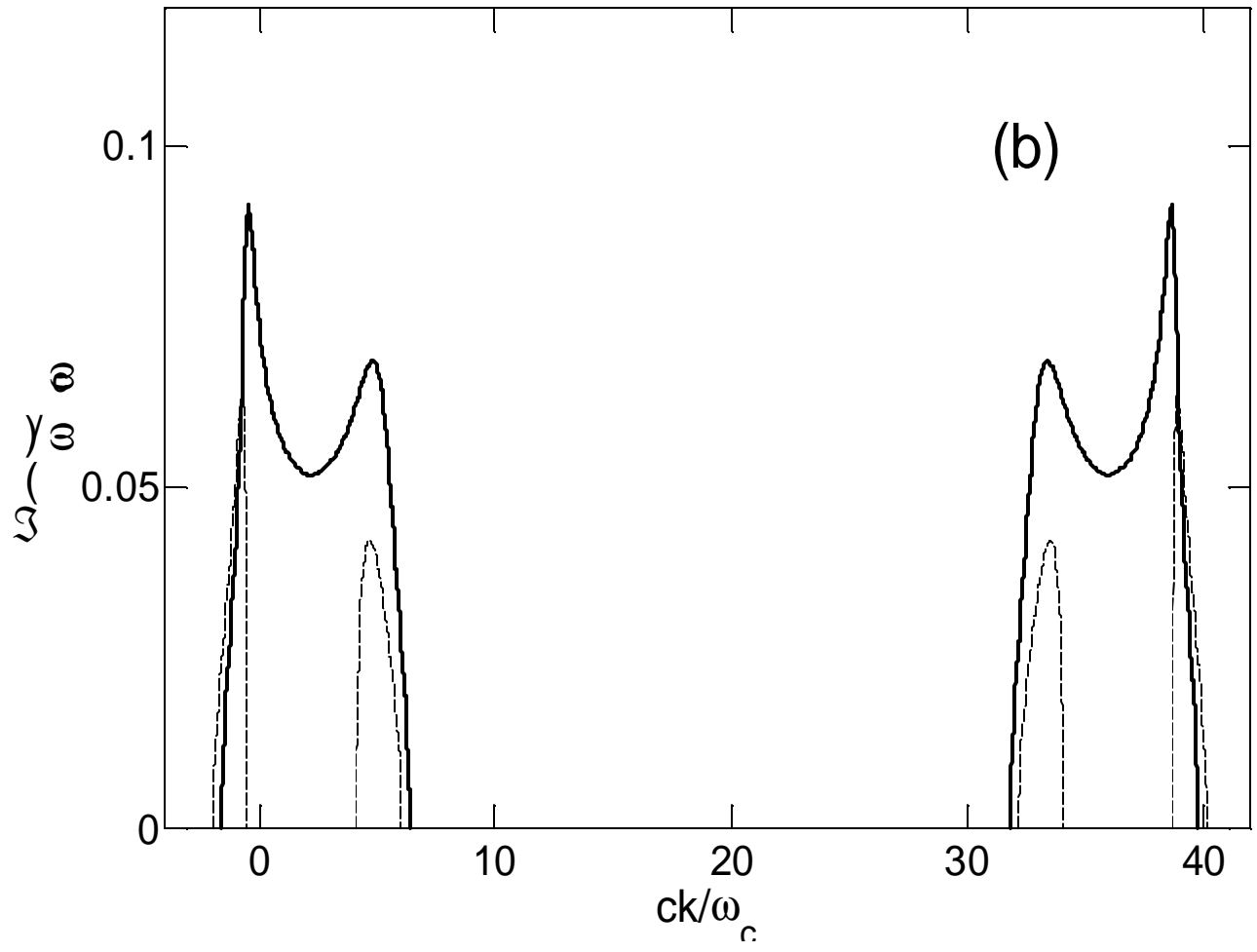


Fig. 3b

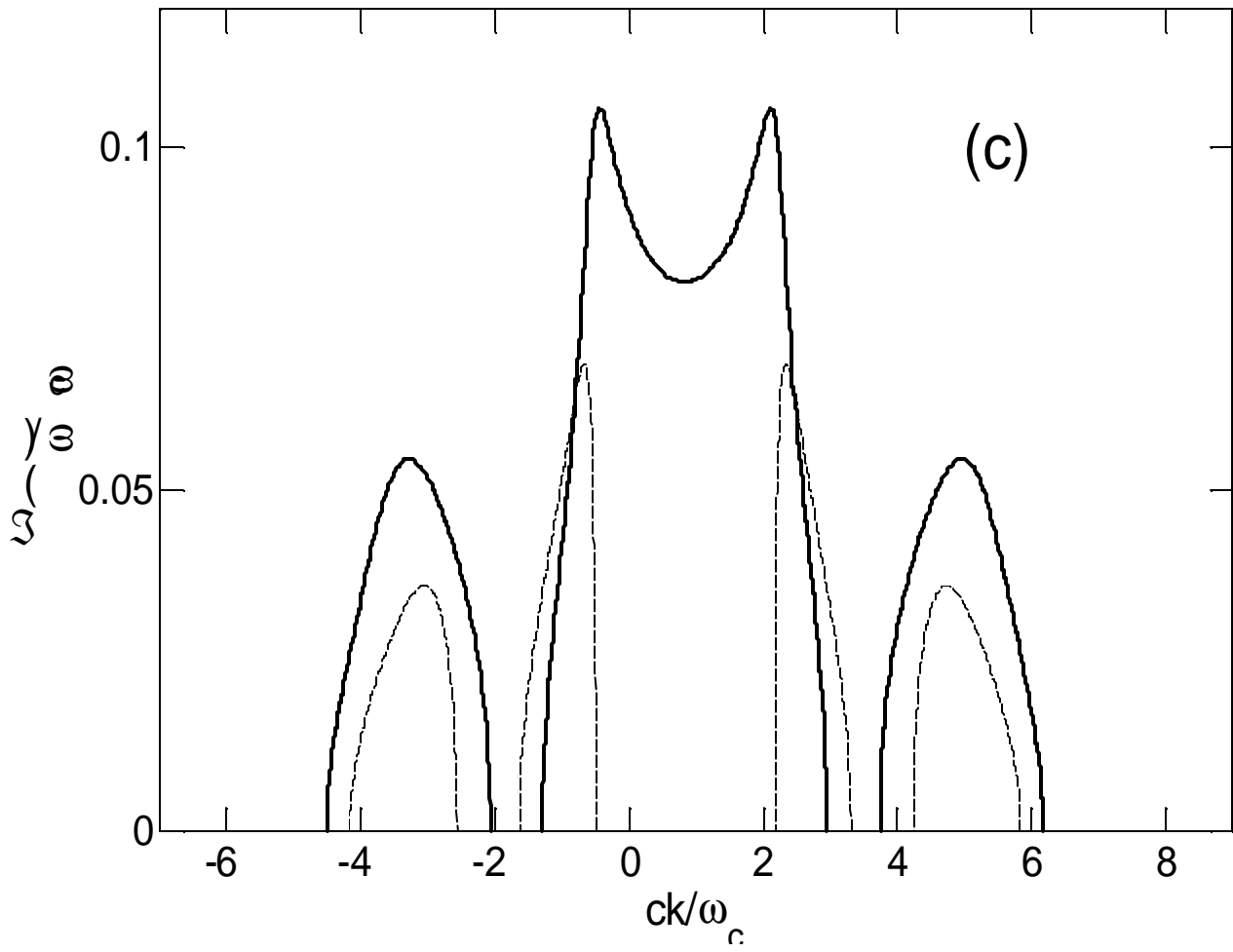


Fig. 3c

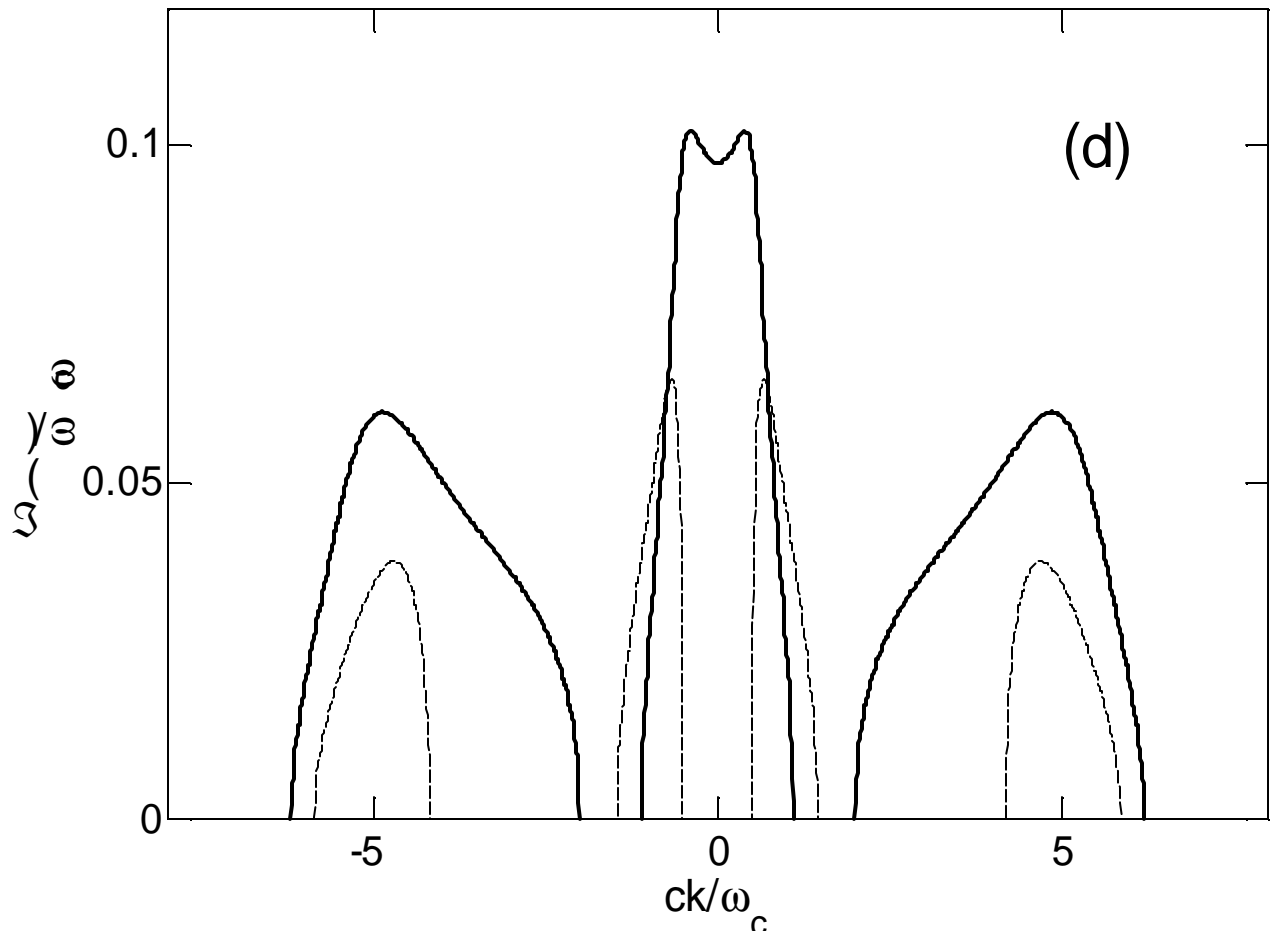


Fig. 3d

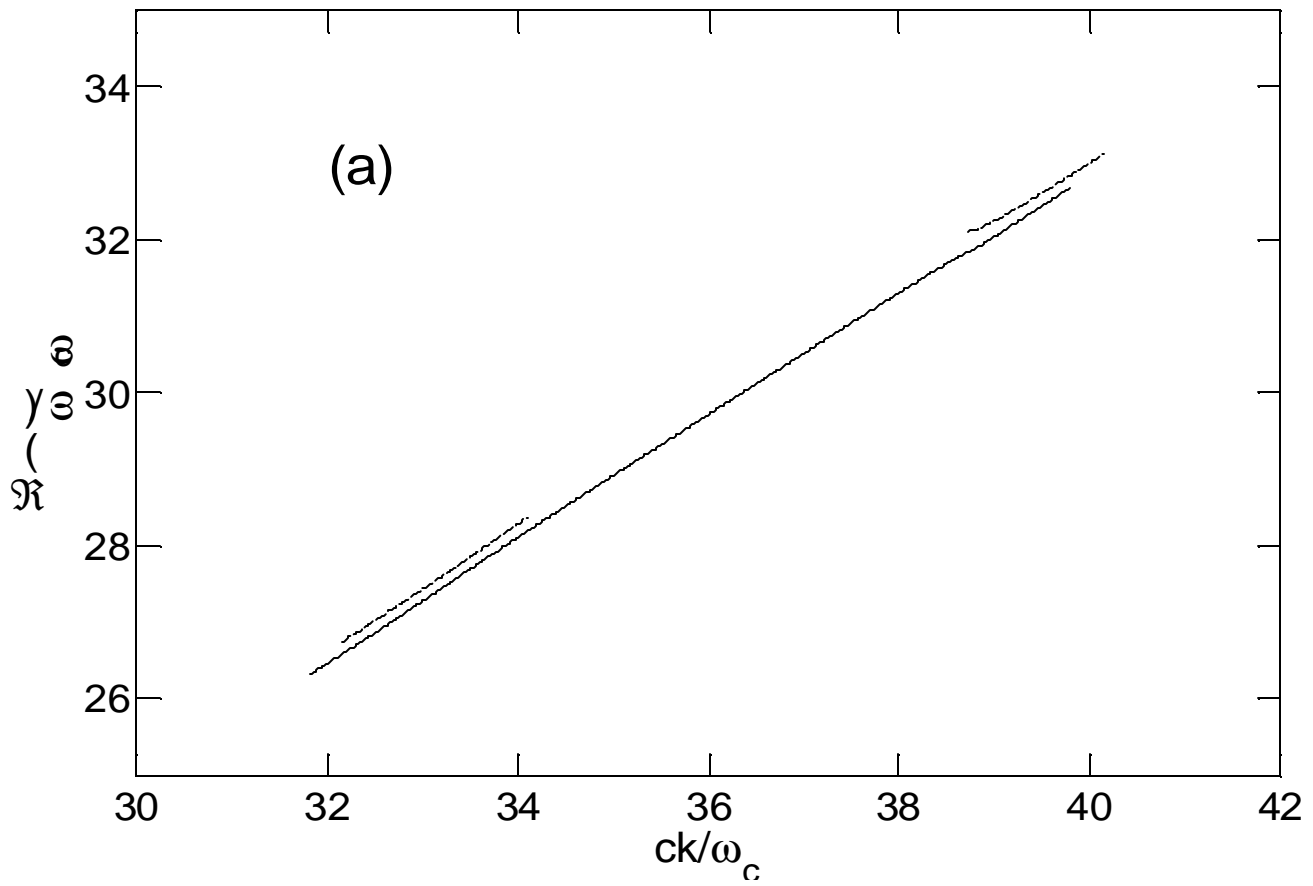


Fig. 4a

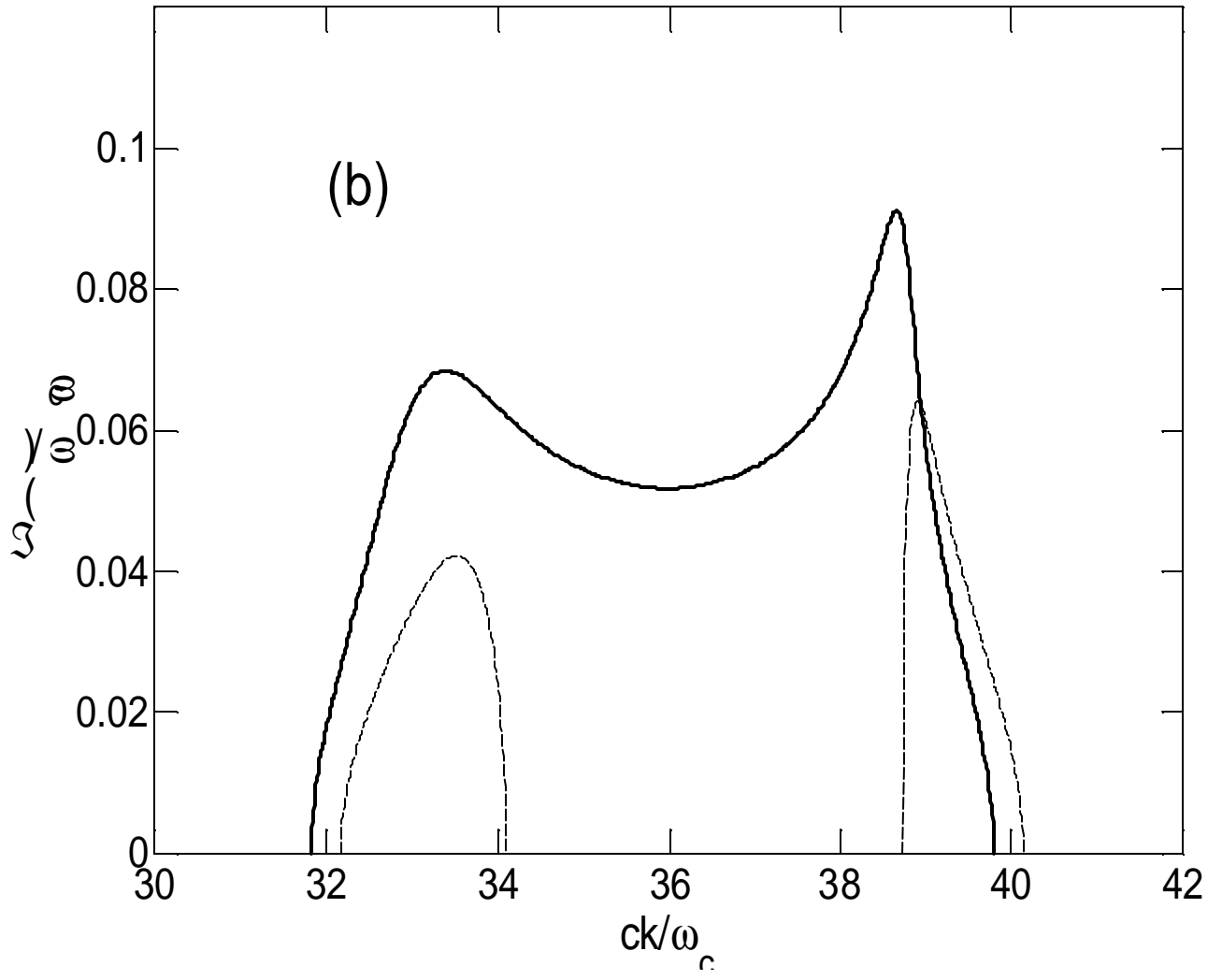


Fig. 4b

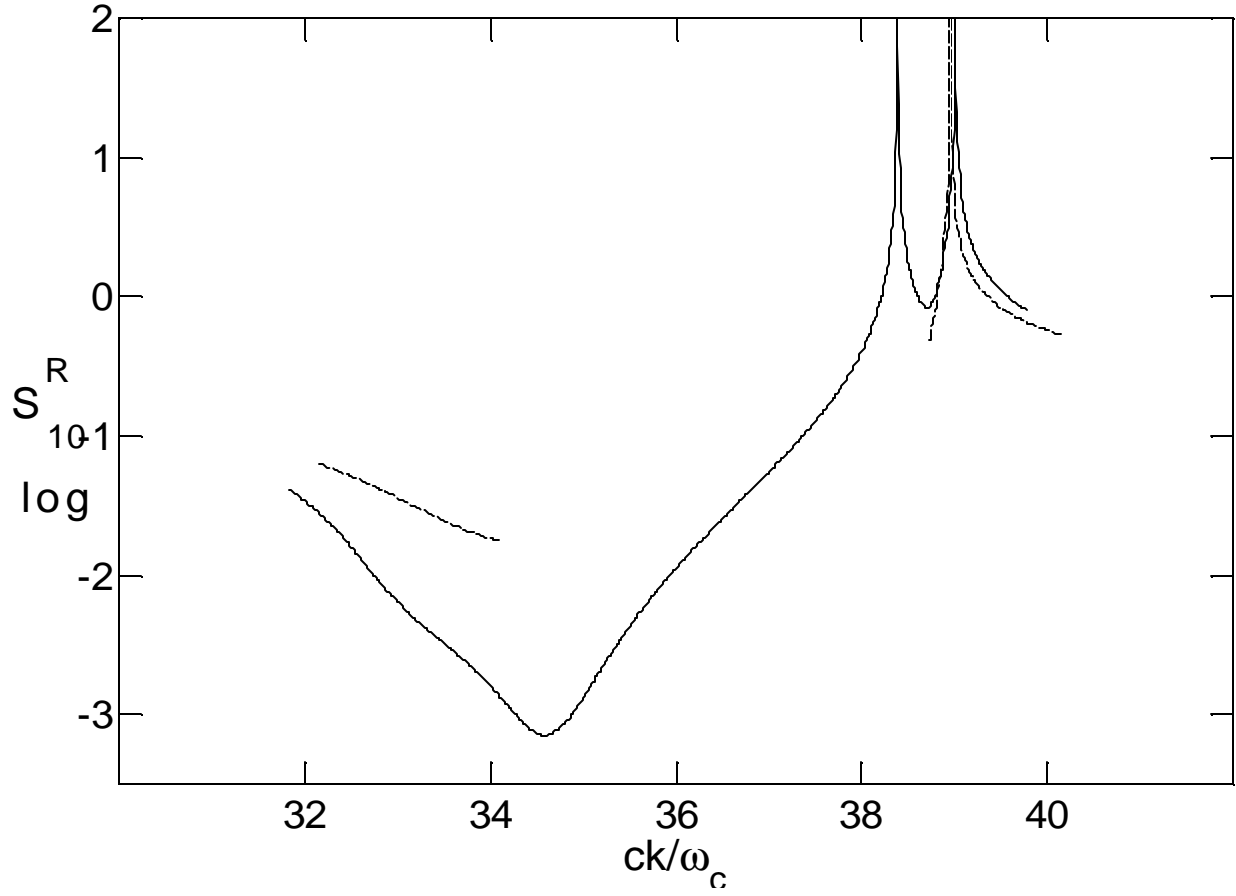


Fig. 5

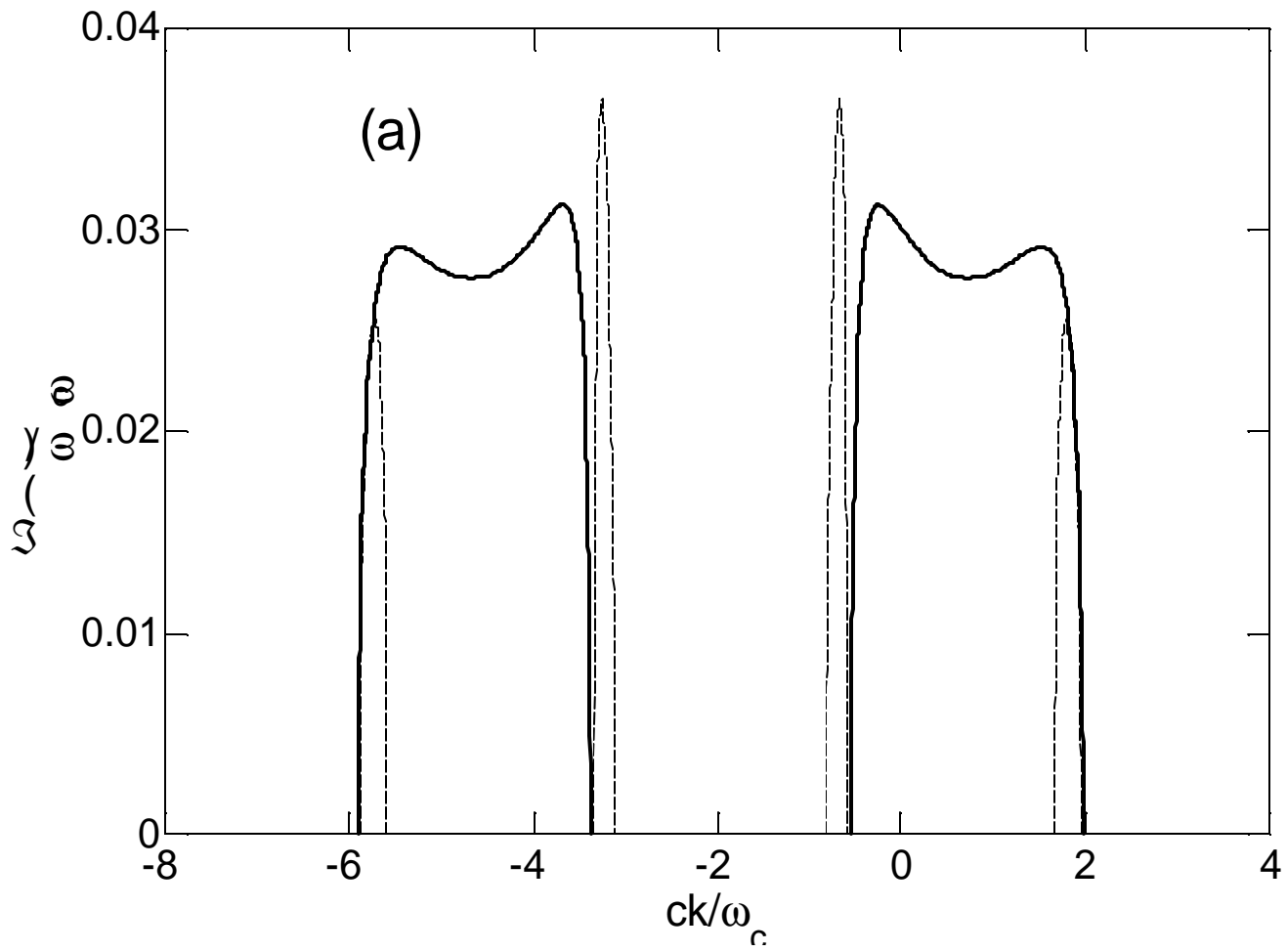


Fig. 6a

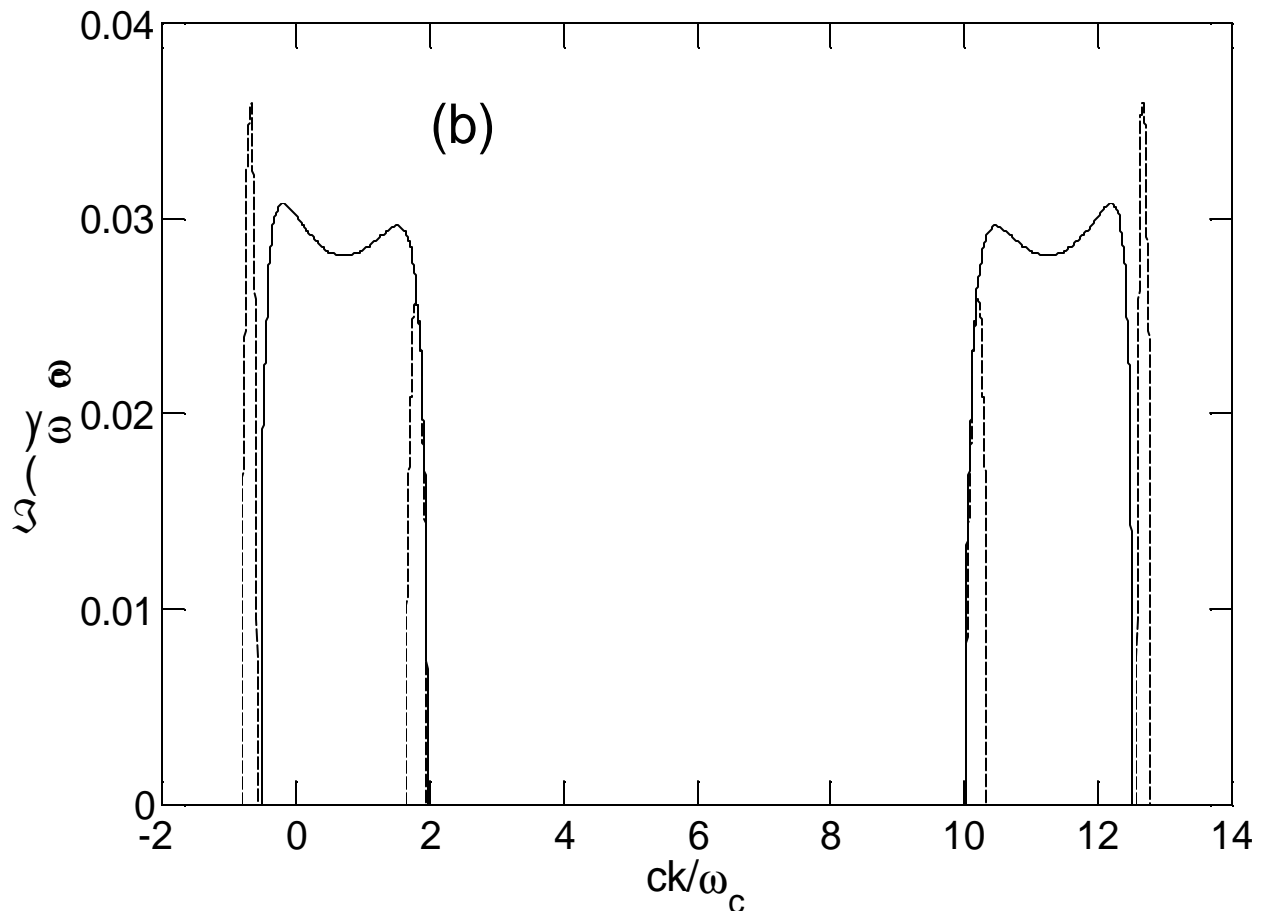


Fig. 6b

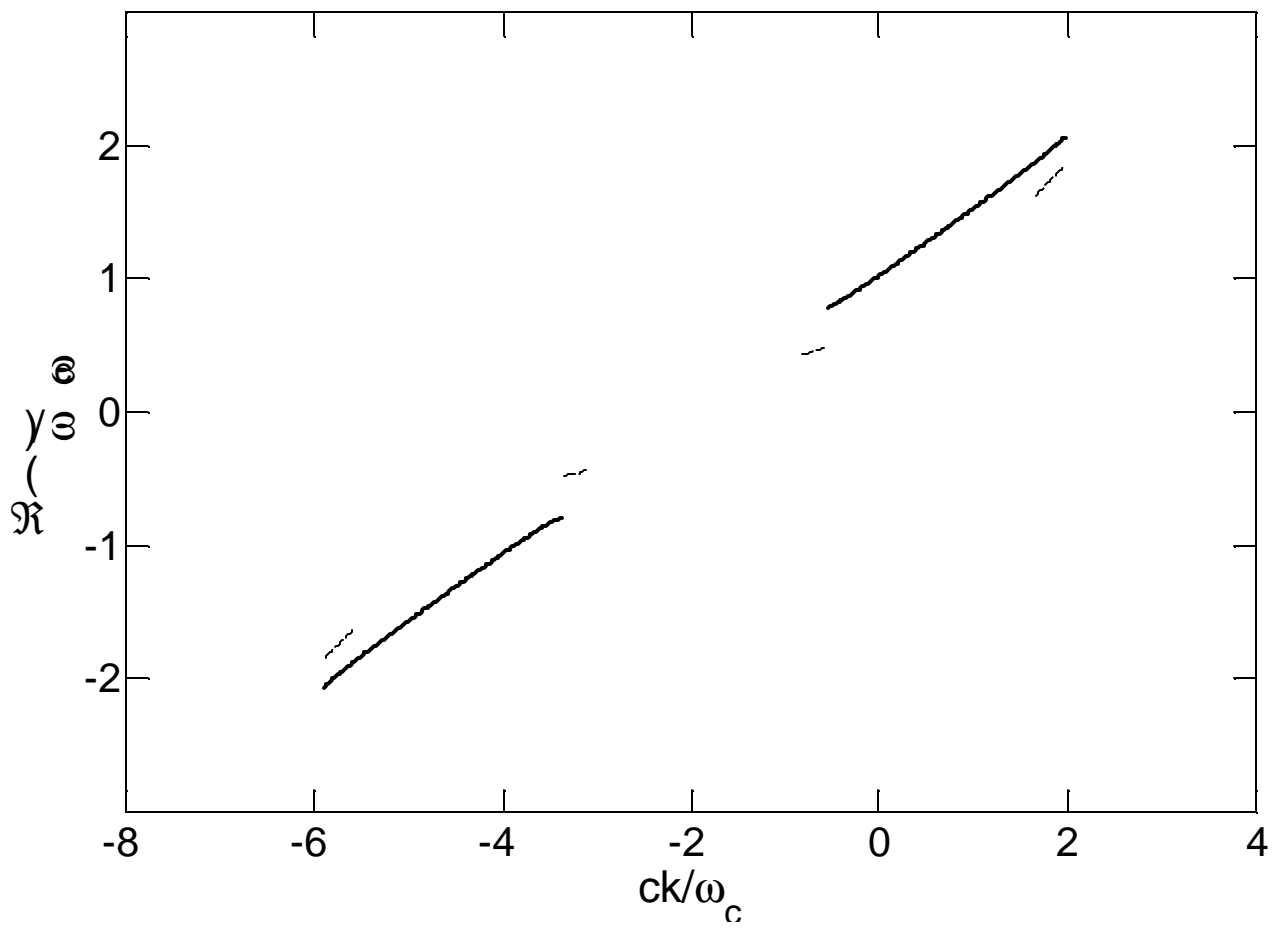


Fig. 7

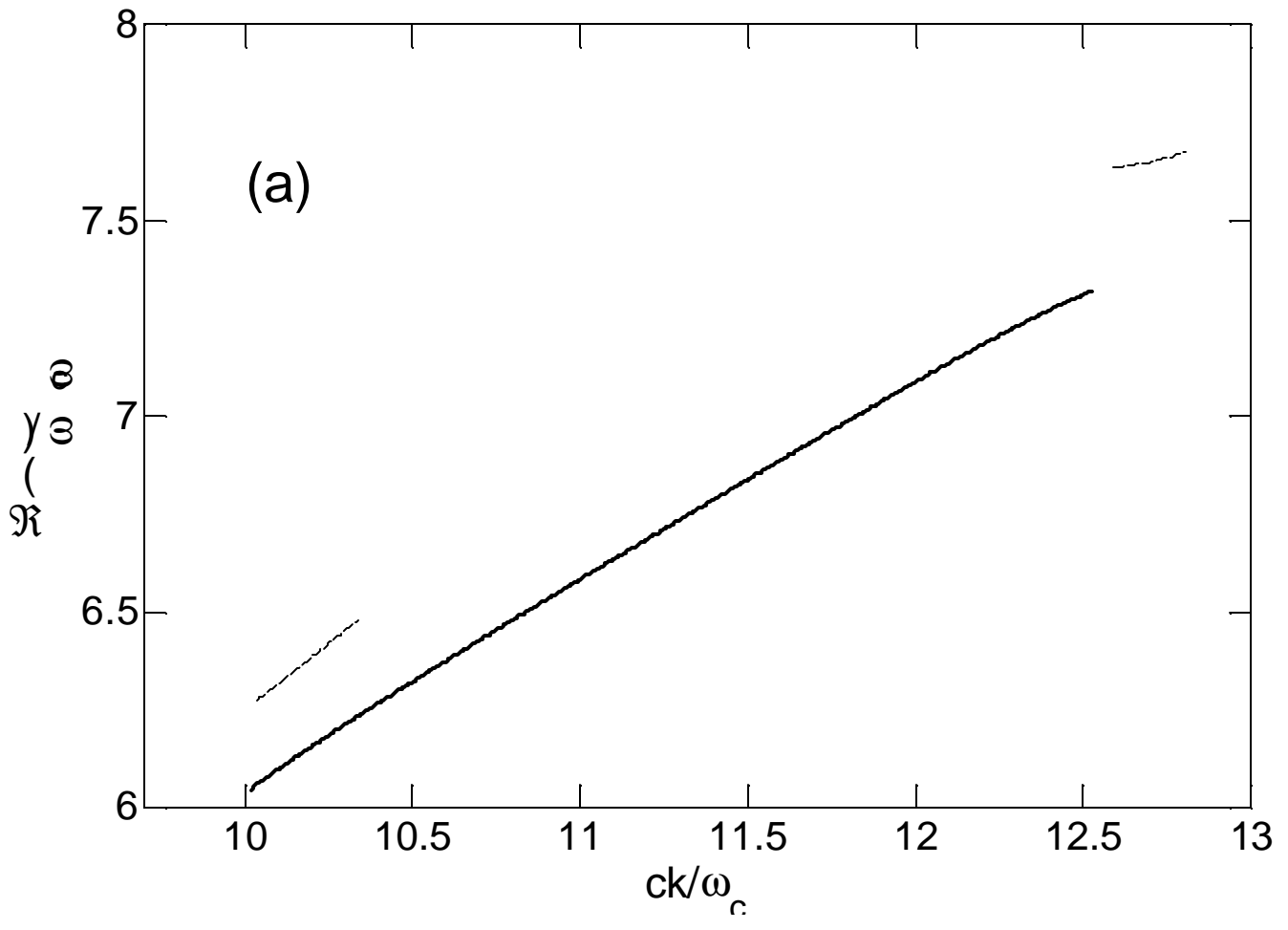


Fig. 8a

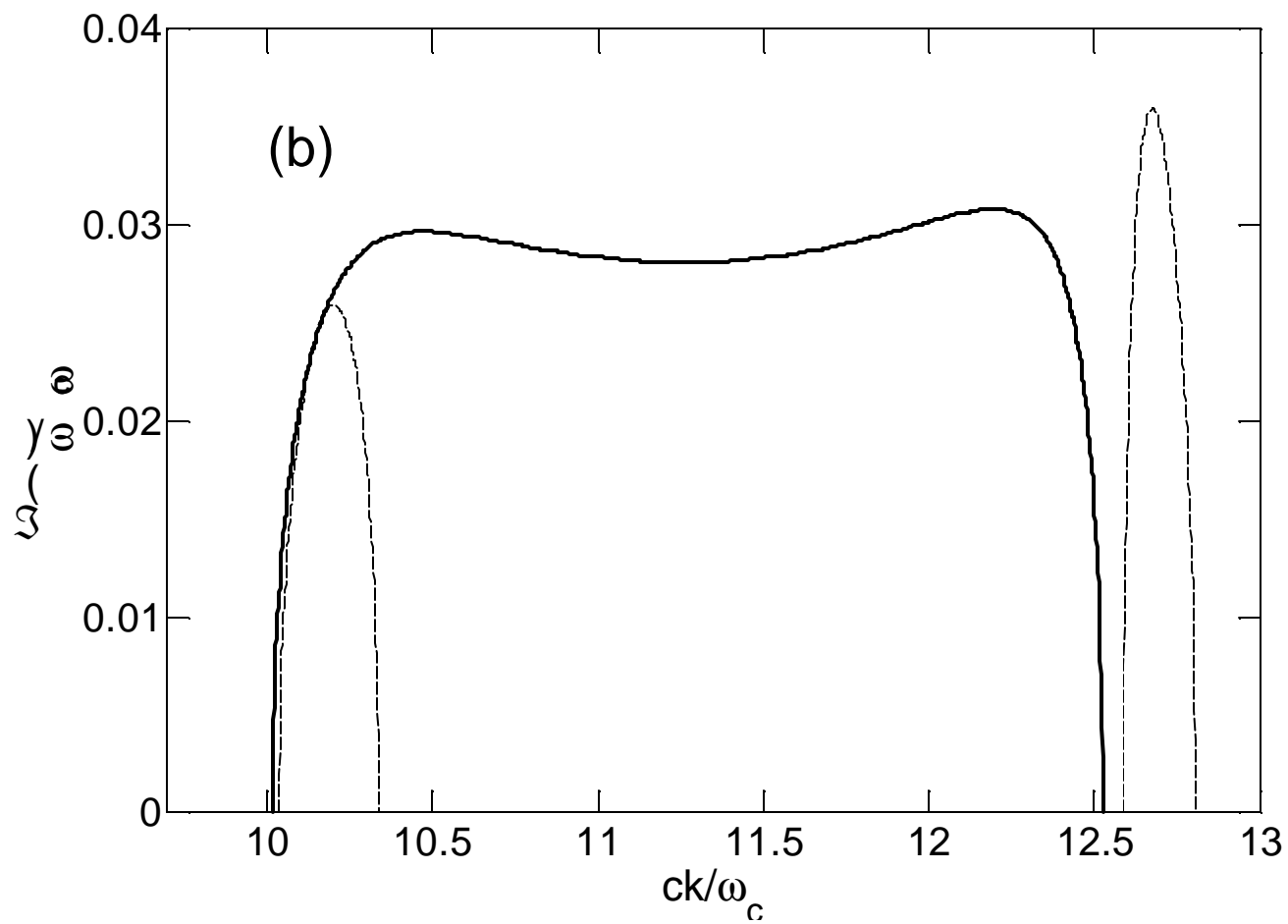


Fig. 8b

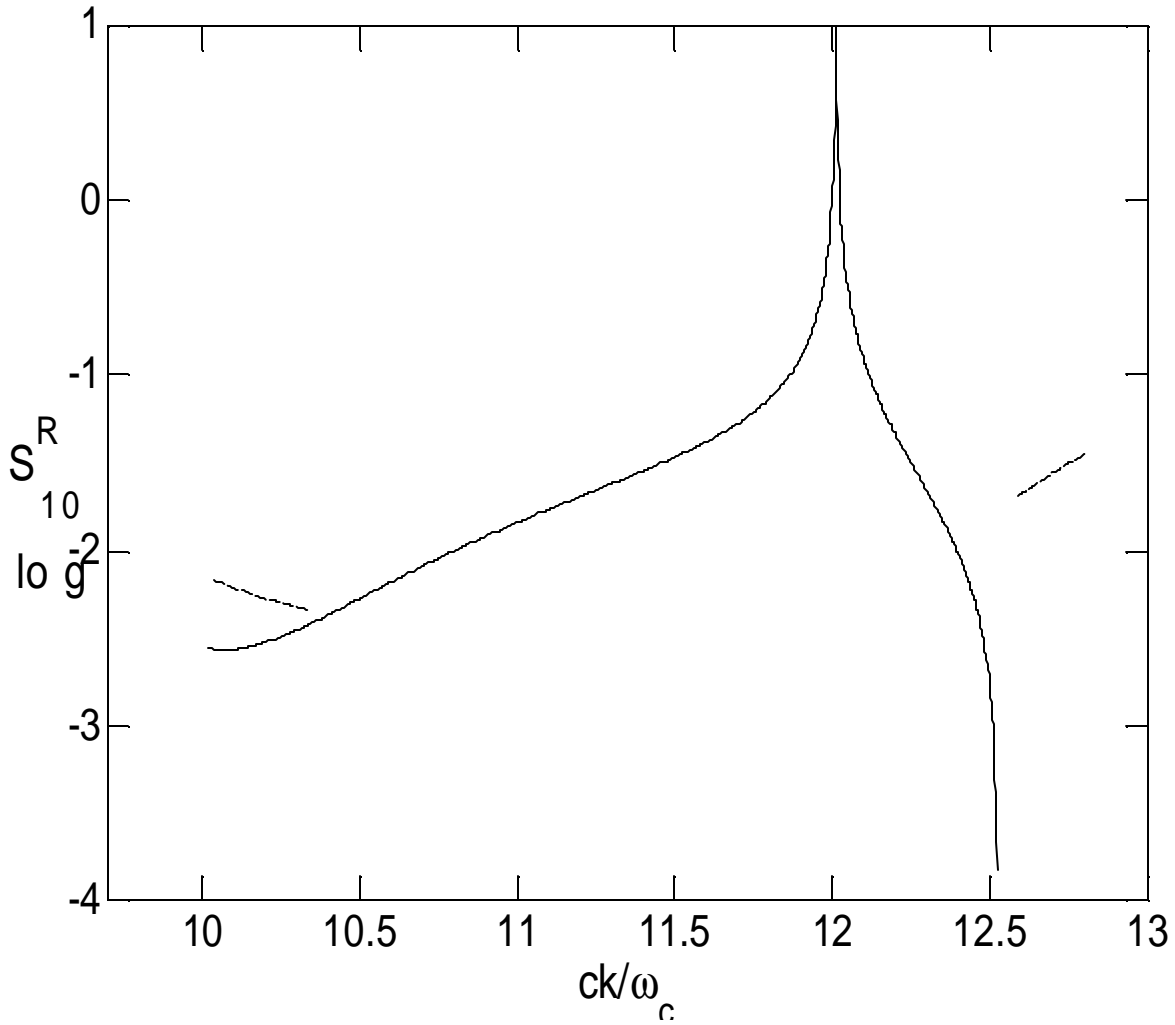


Fig. 9